Recent Results from the Fourier_Quad Shear Measurement Method

Jun Zhang

(Shanghai Jiao Tong University)

KIAS Workshop, Nov 1, 2024

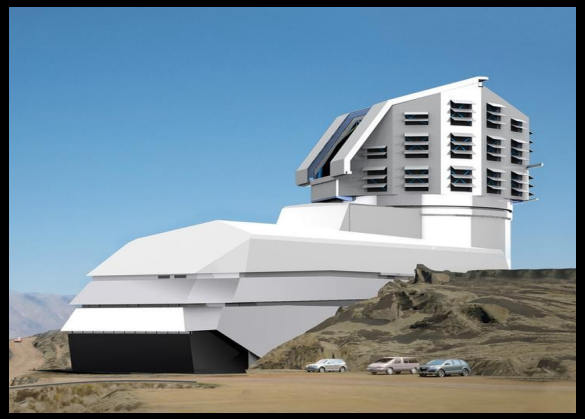
Outline:

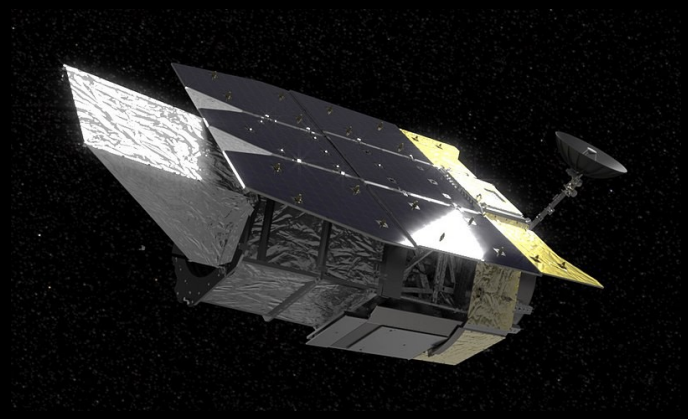
- Motivation & Thoughts
- Recent Progress
- Conclusions

Outline:

- Motivation & Thoughts
- Recent Progress
- Conclusions

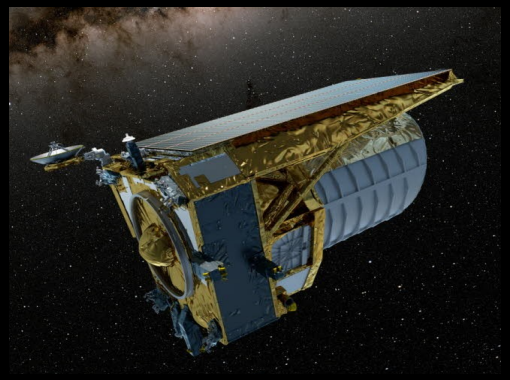
Our Opportunities -- Stage IV Dark Energy Surveys





CSST(CHINA)





HSC	DES	LSST	Euclid	Roman	CSST
2014	2013	2024	2023	2025	~2027
1400deg^2	5000deg^2	18000deg^2	15000deg^2	2700deg^2	17500deg^2
~ 0.1B	~0.3B	~ 2B	~ 1B	~0.3B	~ 1B

Weak Lensing Science

- **Structure Growth**
- **Expansion History**
- **Properties of Dark Matter**
- **Properties of Dark Energy**
- **Tests of Gravity Theories**
- **Density Profiles of Groups and Clusters**
- **Profiles of Filaments, Voids, ...**
- **… … … …**

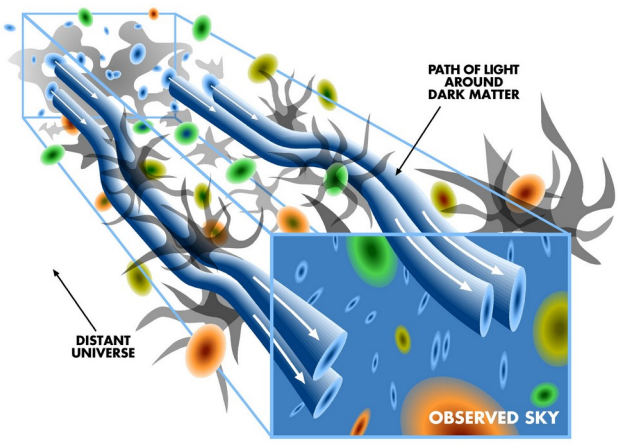
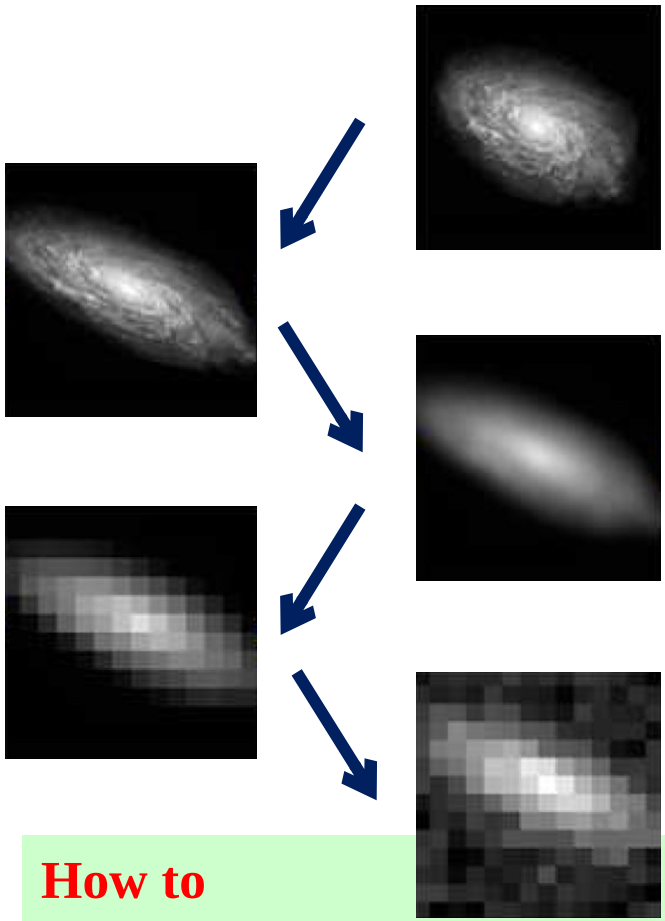


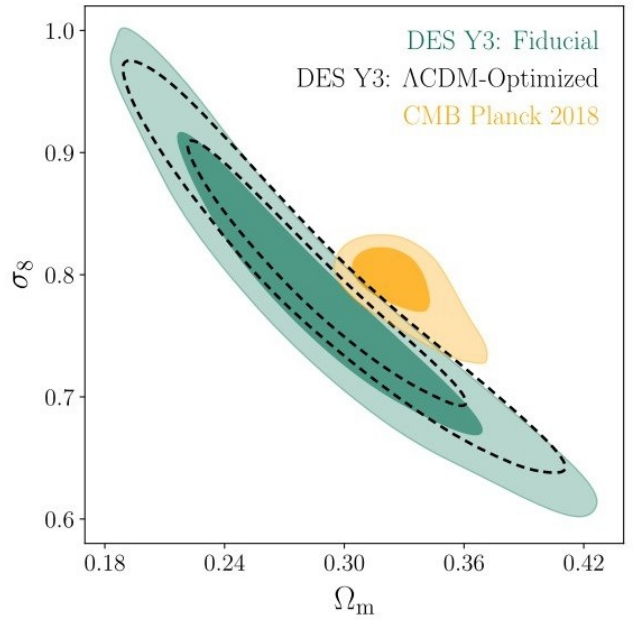
Image credit: Wittman et al. (2000)

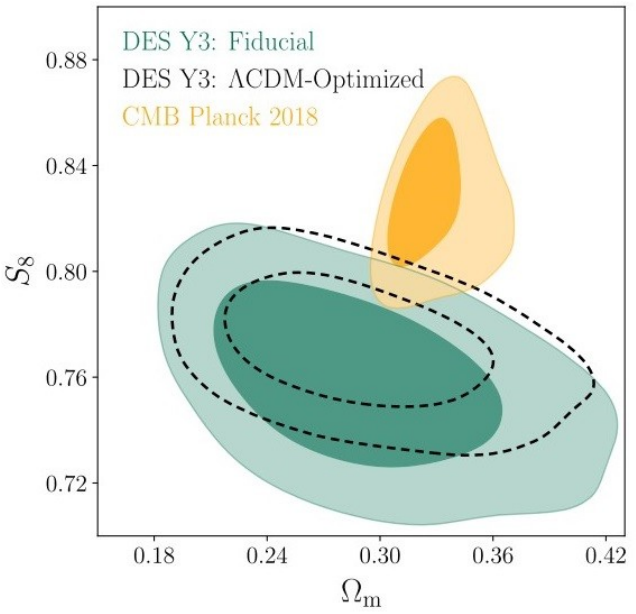
Challenges



How to

achieve high precision shear measurement under general observing conditions?





DES Y3 Results
Amon et al., 2022, PRD, 105, 023514

Different Methods (Mandelbaum et al. 2015 ,GREAT3)

Team	Class	Weighting scheme	Calibration philosophy	Limitations	$N_{\rm branch}$	Rank	Exact PSF?	New software	Time per galaxy
Amalgam@IAP	Maximum likelihood	Inverse variance	Ellipticity penalty	None	16	2	Yes	Some	0.1–1 s
BAMPenn	Bayesian Fourier	Implicit	$p(\varepsilon)$ from deep data	Variable shear	2	-	Yes	Yes	<1 s
EPFL_gfit	Maximum likelihood	Constant + rejection	None	None	8	6	Yes	Yes	1–3 s
CEA-EPFL	Maximum likelihood	Various	None	None	20	3	Yes	Yes	1–3 s
CEA_denoise	Moments	Constant	None	None	8	-	Yes	No	0.03 s
CMU experimenters	Stacking	Constant	External simulations	Variable shear	2	N/A	Yes	Some	0.03 s
COGS (IM3SHAPE)	Maximum likelihood	Constant	External simulations	None	12	N/A	Yes	Yes	1 s
E-HOLICS	Moments	Constant + rejection	External simulations	None	12	8	Yes	No	1–3 s
EPFL_HNN	Neural network	Constant	None	None	7	-	Yes	Yes	2-3 s
EPFL_KSB	Moments	Inverse variance	None	None	4	-	Yes	No	0.001-0.002 s
EPFL_MLP / EPFL_MLP_FIT	Neural network	Constant	None	None	5	-	Yes	Yes	2-3 s
FDNT	Fourier moments	Inverse variance	External simulations	None	12	N/A	Yes	Some	~ 1 s
Fourier_Quad	Fourier moments	Various	None	None	6	5	Yes	No	0.001-0.002 s
HSC/LSST-HSM	Moments	Inverse variance	External simulations	None	4	N/A	Yes	Some	0.05 s
MBI	Bayesian hierarchical	Implicit	Inferred $p(\varepsilon)$	Variable shear, PSF	4	9	No	Some	10 s
MaltaOx (LENSFIT)	Partially Bayesian	Inverse variance	Self-calibration	None	3	7	Yes	Some	0.05 s
MegaLUT	Supervised ML	Constant + rejection	External simulations	None	16	4	Yes	Some	0.02 s
MetaCalibration	Moments + self-calibration	Inverse variance	Self-calibration	Variable shear	1	N/A	Yes	Yes	0.3 s
Wentao_Luo	Moments	Inverse variance	None	None	4	-	Yes	Yes	1-2 s
ess	Bayesian model-fitting	Implicit	$p(\varepsilon)$ from deep data	Variable shear	2	-	No	Yes	1 s
sFIT	Maximum likelihood	Inverse variance	External simulations (iterative)	None	20	1	Yes	Yes	0.8 s



Measuring the Cosmic Shear in Fourier Space

Jun Zhang (张骏)

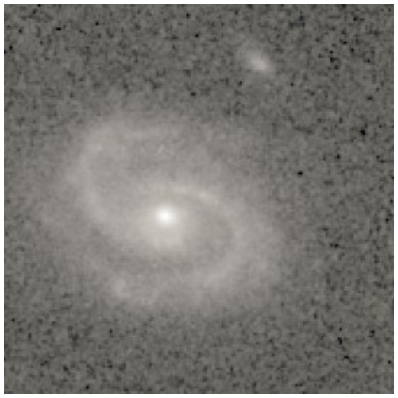
(Shanghai Jiao Tong University)

Collaborators:

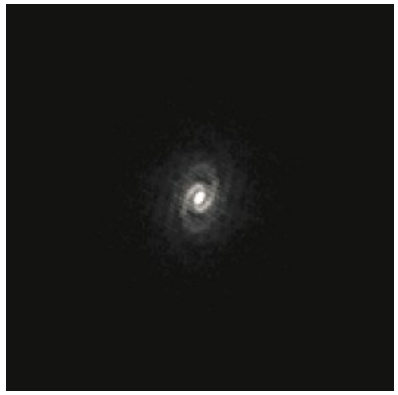
Eiichiro Komatsu (MPA), Nobuhiko Katayama (IPMU), Wentao Luo (SHAO), Sebastian Foucaud (SJTU)

References:
JZ, 2008, MNRAS, 383, 113
JZ, 2010, MNRAS, 403, 673
JZ & Komatsu, 2011, MNRAS, 414, 1047
JZ, 2011, JCAP, 11, 041
JZ, Luo, Foucaud, 2013, arXiv:1312.5514

The Fourier_Quad Shear Estimator



$$\widetilde{f}(\vec{k}) = \int d^2\vec{x} e^{i\vec{k}\cdot\vec{x}} f(\vec{x}).$$



$$G_1 = -\frac{C}{2}\sum_{j=1}^{N_T}\left[(\vec{k}_j)_x^2 - (\vec{k}_j)_y^2\right] T(\vec{k}_j) M(\vec{k}_j)$$

$$G_2 = -C\sum_{j=1}^{N_T}(\vec{k}_j)_x(\vec{k}_j)_y T(\vec{k}_j) M(\vec{k}_j)$$

$$N = C\sum_{j=1}^{N_T}\left[\left|\vec{k}_j\right|^2 - \frac{\beta^2}{2}\left|\vec{k}_j\right|^4\right] T(\vec{k}_j) M(\vec{k}_j)$$

$$\frac{\langle G_1\rangle}{\langle N\rangle} = g_1, \qquad \frac{\langle G_2\rangle}{\langle N\rangle} = g_2$$

$$M(\vec{k}) = \left|\tilde{f}^O(\vec{k})\right|^2 - F^O - \left|\tilde{f}^B(\vec{k})\right|^2 + F^B$$

$$F^O = \frac{\sum_{|\vec{k}_j|>k_c}\left|\tilde{f}^O(\vec{k}_j)\right|^2}{\sum_{|\vec{k}_j|>k_c}}, \qquad F^B = \frac{\sum_{|\vec{k}_j|>k_c}\left|\tilde{f}^B(\vec{k}_j)\right|^2}{\sum_{|\vec{k}_j|>k_c}}$$

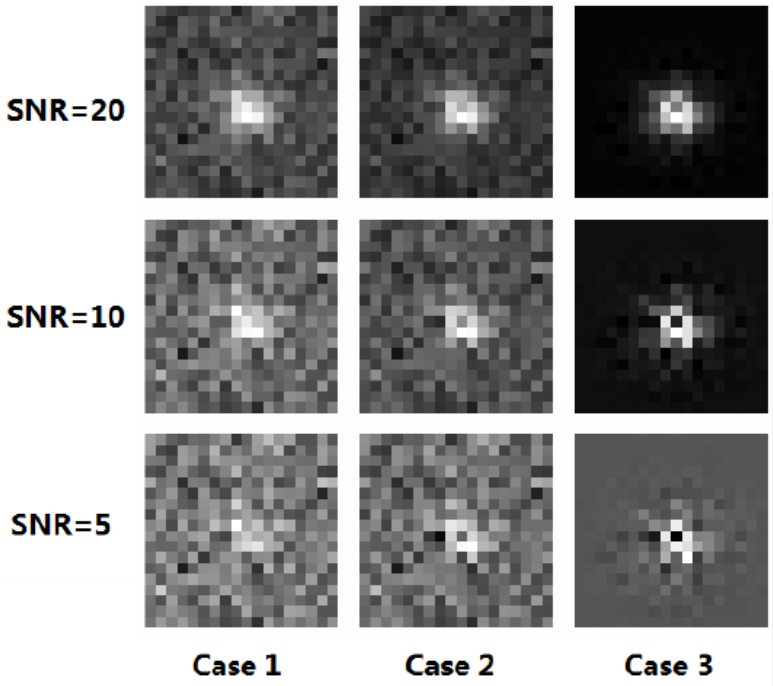
$$T(\vec{k}_j) = \left|\tilde{W}_\beta(\vec{k}_j)\right|^2 / \left|\tilde{W}_{PSF}(\vec{k}_j)\right|^2$$

JZ et al., 2015, JCAP, 1, 24

Test Results

$$g_1^{measured} = (1+m_1)g_1^{input} + c_1$$

$$g_2^{measured} = (1+m_2)g_2^{input} + c_2$$



	Case 1	Case 2	Case 3
SNR= 20	$m_1(10^{-3}) : -0.2 \pm 0.2$	-0.2 ± 0.1	-0.08 ± 0.05
	$c_1(10^{-5}) : -1.0 \pm 0.7$	-0.6 ± 0.4	0.0 ± 0.2
SNR= 10	-0.6 ± 0.6	-0.4 ± 0.4	-0.1 ± 0.1
	-2.6 ± 2.1	-1.6 ± 1.2	0.0 ± 0.4
SNR= 5	-2.2 ± 2.3	-1.1 ± 1.2	0.0 ± 0.2
	-7.9 ± 7.9	-4.6 ± 4.1	0.1 ± 0.8
SNR= 20	$m_2(10^{-3}) : -0.2 \pm 0.2$	-0.3 ± 0.1	-0.3 ± 0.05
	$c_2(10^{-5}) : 1.4 \pm 0.7$	1.1 ± 0.4	0.3 ± 0.2
SNR= 10	-0.3 ± 0.6	-0.4 ± 0.4	-0.4 ± 0.1
	3.7 ± 2.1	2.6 ± 1.2	0.6 ± 0.4
SNR= 5	-0.7 ± 2.3	-0.9 ± 1.2	-0.6 ± 0.2
	10.6 ± 7.9	6.6 ± 4.1	1.2 ± 0.8

JZ et al., 2015, JCAP, 1, 24

Some Thoughts

- How do we know our measurement on real data is really accurate? Or, could we directly calibrate the shear bias using the data itself ?
- Are we really limited by the seeing size?
- Can shape measurement be carried out in all bands?
- Do we need to specify individual source of systematic errors?

Are the current mock simulations complicated enough?

redshift inference as is performed on the real data, allowing reliable and consistent corrections for each photometric redshift bin.

While we believe these simulations are sufficiently realistic given the requirements of the DES Year 3 cosmology analyses, they do of course involve approximations and shortcuts that may not be sufficiently accurate for future analyses. We do not simulate the estimation of the WCS solution, PSF, background levels or noise levels in our simulations, under the assumption that any errors in our estimation of these in the real data are negligible. These assumptions should be carefully re-examined for more precise upcoming weak lensing data sets.

In addition, we simulated galaxies with random sky positions, rather than a realistic level of clustering. While our re-weighting

MacCrann et al. (DES), 2022

Are the current mock simulations complicated enough?

We recognise that our simulations will need further elements of realism. First, we have shown initial results for nominal simulation settings and have studied the sensitivity to some key parameters. This proves essential in order to break down the bias in its main contributions, but it does not give us an exhaustive answer to the full calibratability of our method. While we have tested the sensitivity to some key effects, we will need to carry out a more thorough study of the sensitivity to choices made in SourceXtractor++ (e.g., detection thresholds and convolution filter) and the distribution of faint galaxies. Furthermore, we have shown results for models that match those in the simulations for three parameters (see fixed ones in Table 1) and then also after relaxing assumptions made for bulges. The residual bias is still under control and its sensitivity is weak, but more parameters will need to be varied in a follow-up work. Another point of future work is the inclusion of cosmic rays, which are identified as one of the main causes of concern for space-base lensing surveys. In fact, while these are usually masked out at detector level, residuals and undetected cosmic rays may still impact the shear measurement significantly. Similarly, detector non-linearities, CTI, and BFE have not been included and while again there are already strategies to correct for those at detector level, residuals should still be fully propagated through. A complete study of redshift dependent biases is a further essential step, where it will also be necessary to account for the colour dependence (leading to an effective redshift dependence) of the PSF modelling. As the PSF modelling is a strong function of both colour and redshift, future realistic simulations that include tomographic binning will also have to include the full spatial and colour variability of the galaxies. Closely related, galaxy colour gradients[32] might lead to additional redshift-dependent biases (Semboloni et al. 2013; Er et al. 2018).

Congedo et al. (EUCLID), 2024

Outline:

- Motivation & Thoughts
- Recent Progress
- Conclusions

Overview of our Progress in Shear Measurement

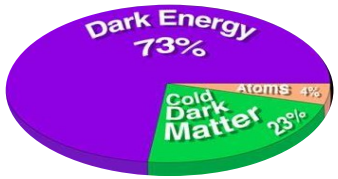
- ApJ,875,48(2019)： Pipeline construction， applied on the CFHTLenS data
- AJ,164,128(2022)： Pipeline improvement， applied on the DECaLS data
- arXiv:2407.00370： Pipeline improvement， applied on the HSC data



Raw Images → Background Removal, Defects Detection → Astrometric Calibration → (PSF) Star Selection → PSF Reconstruction → Self-Calibration Methods

- ApJ,936,161(2022)： Halo Properties & Mass Function Measurement
- MNRAS,513,4754(2022): Halo Depletion Radius Measurement
- arXiv:2408.07373: Ellipticities of Galaxy Cluster Halos from Halo-Shear-Shear Correlations

- AJ,153,197(2017)： PSF reconstruction
- ApJ,858,122(2018)： Correction for the PSF residuals
- ApJ, 972, 120(2024): Correction for Persistent PSF Residuals on the Focal Plane



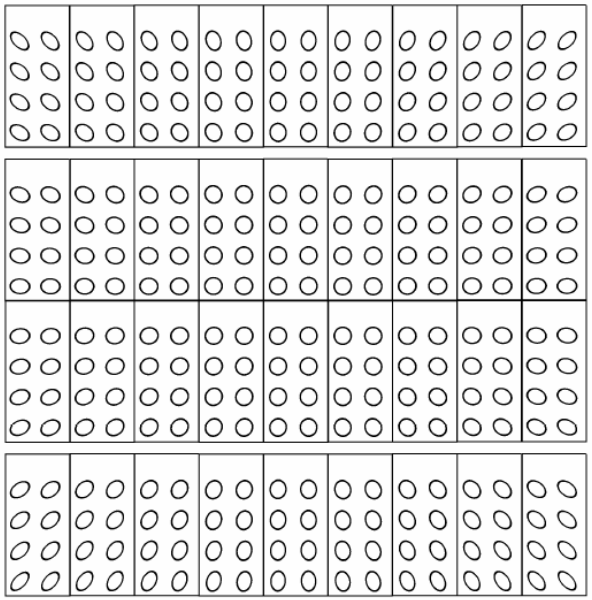
Cosmology & Halo Properties ← Shear Statistics and Optimization ← Shear Catalog ← Shear Measurement with Fourier_Quad

- ApJ,834,8(2017)： Approaching the Cramer-Rao Bound on the Shear Statistics
- ApJ,874,7(2019): A Novel Way of Probing the Lensing Effect of the Low Density Regions
- ApJ,883,155(2019): Avoiding the Eddington Bias in Halo Mass Function Measurement
- ApJ, 954, 193(2023): Optimal Reconstruction of the Shear Field from the Shear Catalog
- SCPMA, 67, 7(2024): Quasi-2D Weak Lensing Statistics
- arXiv:2406.17991: Tele-Correlation as a Way of Calibrating Shear-Shear Correlation with Real Data

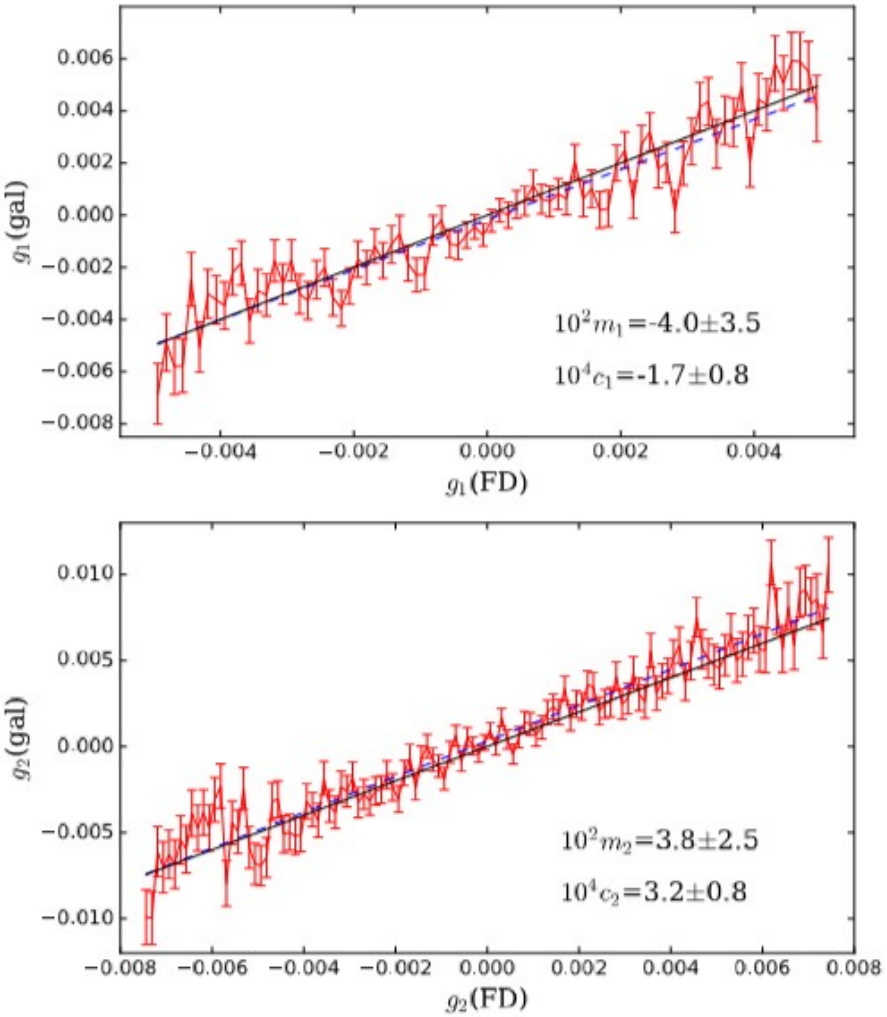
- MNRAS,383,113(2008)： Proposal of the FQ Method
- MNRAS,403,673(2010)： Correction for the Background Noise
- JCAP,11,041(2011)： High Order Corrections
- MNRAS,414,1047(2011)： Form of the Shear Statistics
- JCAP,01,024(2015)： Correction for the Source Poisson Noise
- ApJ,908,93(2021)： Selection Effects
- ApJ,911,10(2021)： Geometric Boundary Effect
- ApJ,911,115(2021)： Source-Noise Coupling Effect

Test Shear Recovery with Field Distortion



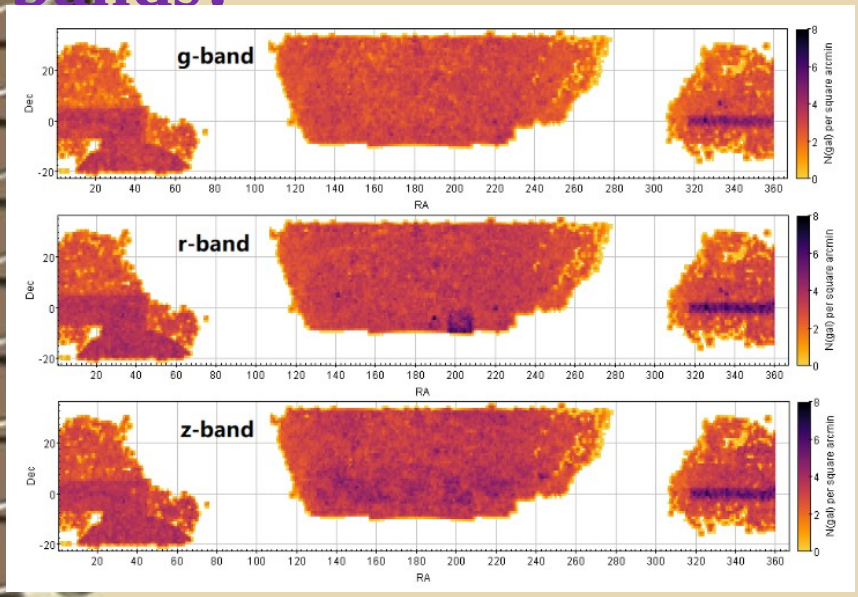


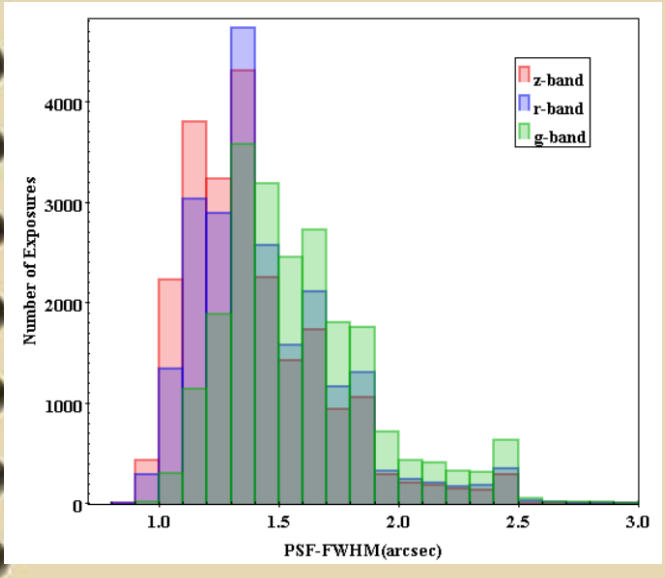
FD distribution on MegaCam, enlarged by 30 times.

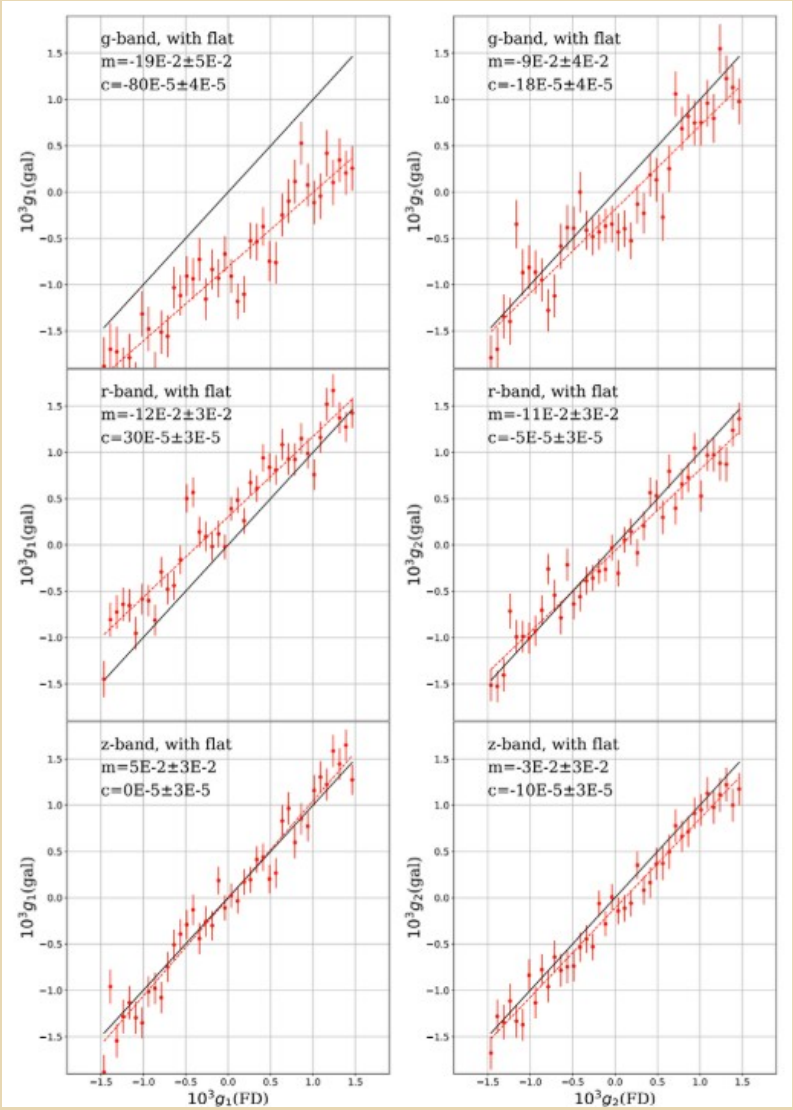


JZ, et al. , 2019, ApJ, 875, 48

Can shape measurement be carried out in all bands?

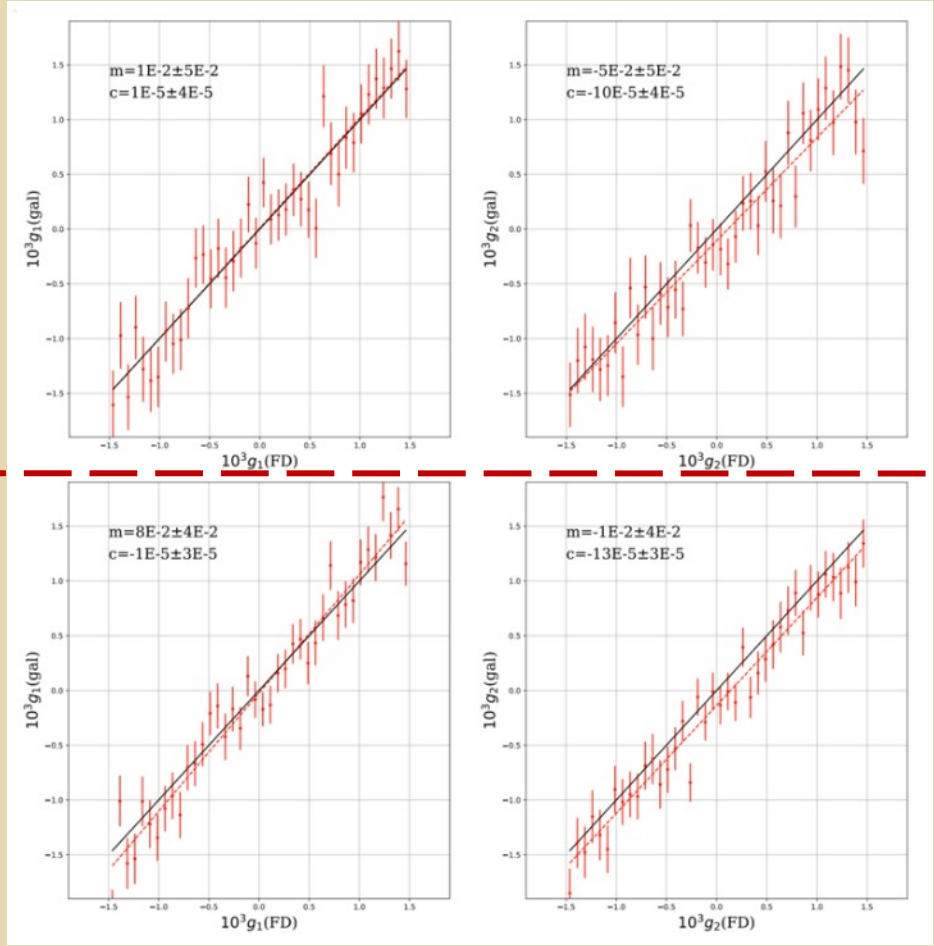




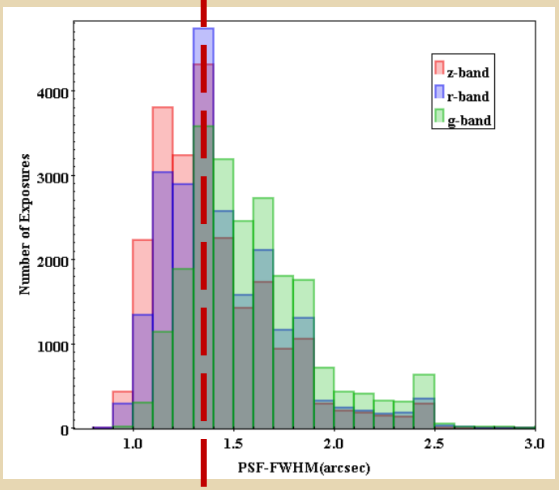


JZ et al., 2022, AJ, 164, 128

Are we really limited by the seeing size?



> 1.4”

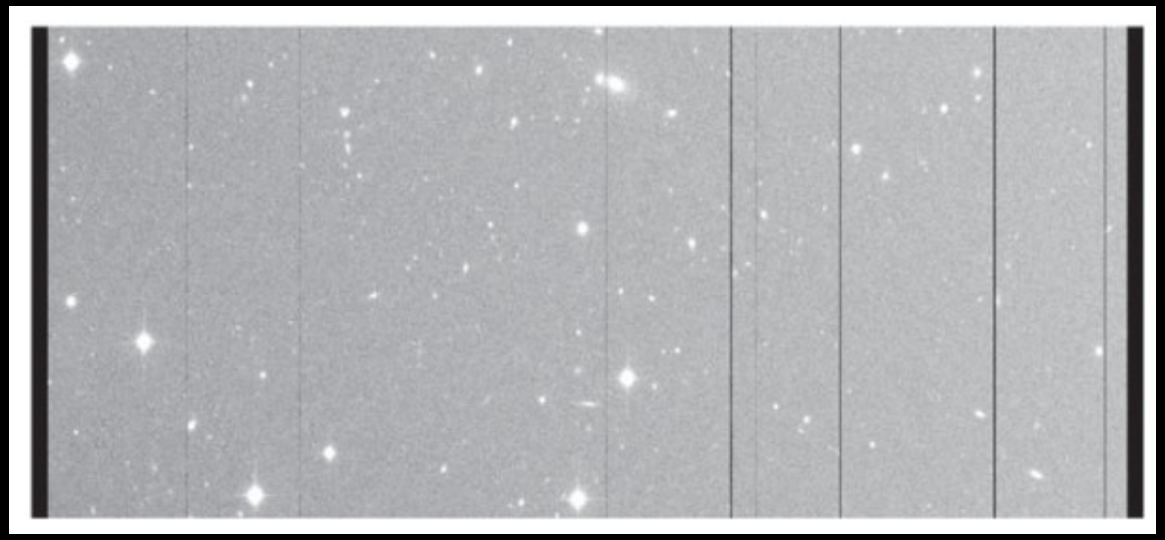


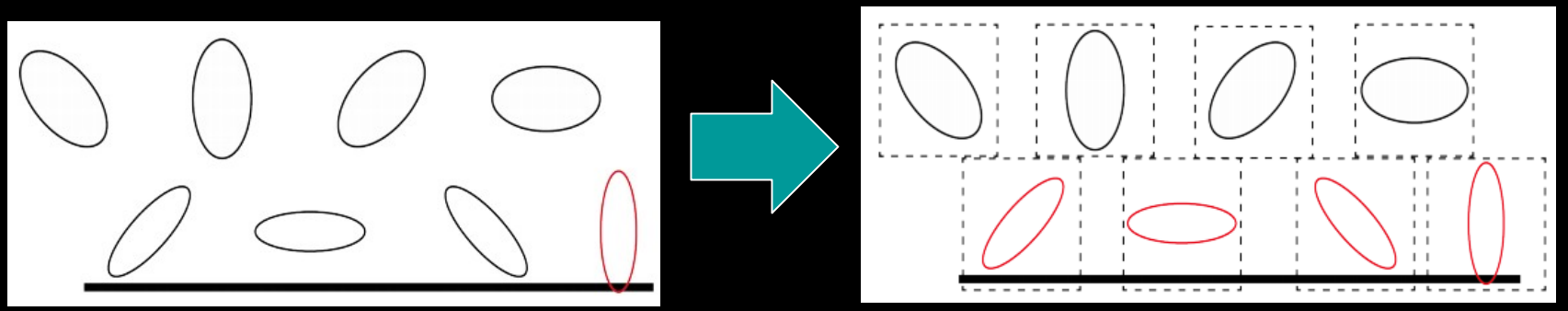
< 1.4”

JZ et al., 2022, AJ, 164, 128

Do we need to specify individual source of systematic errors?

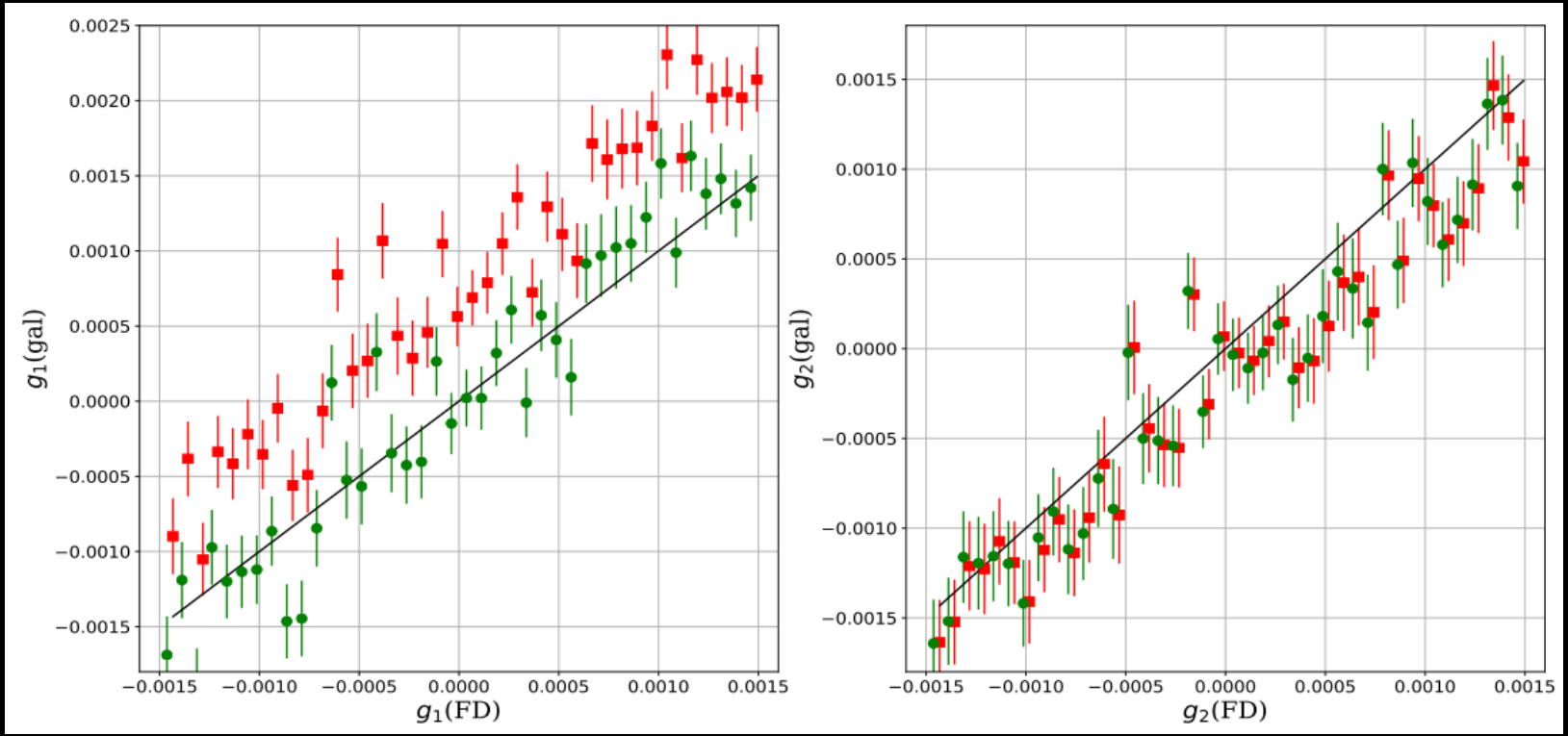
Systematic Error due to Geometrical Boundary





Wang et al., 2021, ApJ, 911, 10

Systematic Error due to Geometrical Boundary



Wang et al., 2021, ApJ, 911, 10

HSC-DR3 Data Processing

Using Fourier_Quad Pipeline, we have finished processing the imaging data of HSC-DR3 with high quality.



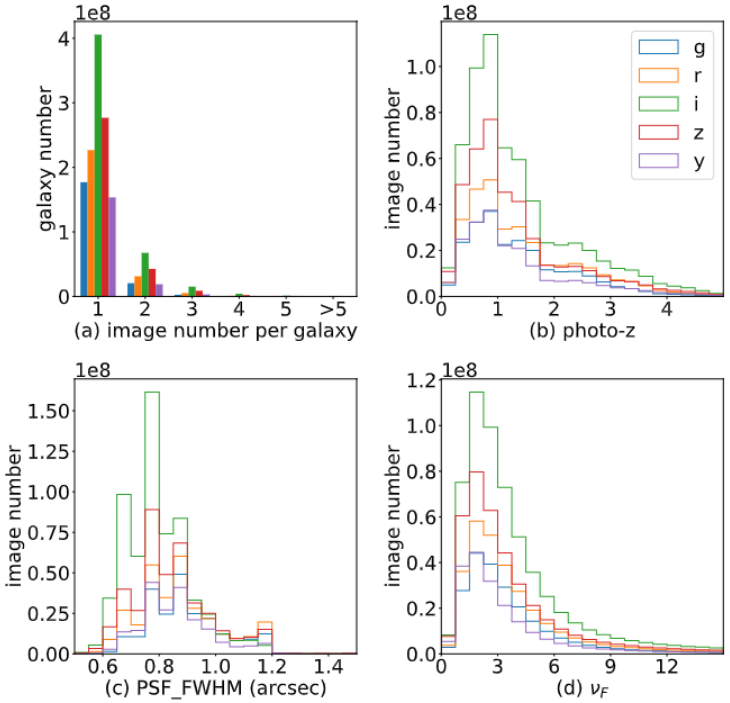
Cong Liu

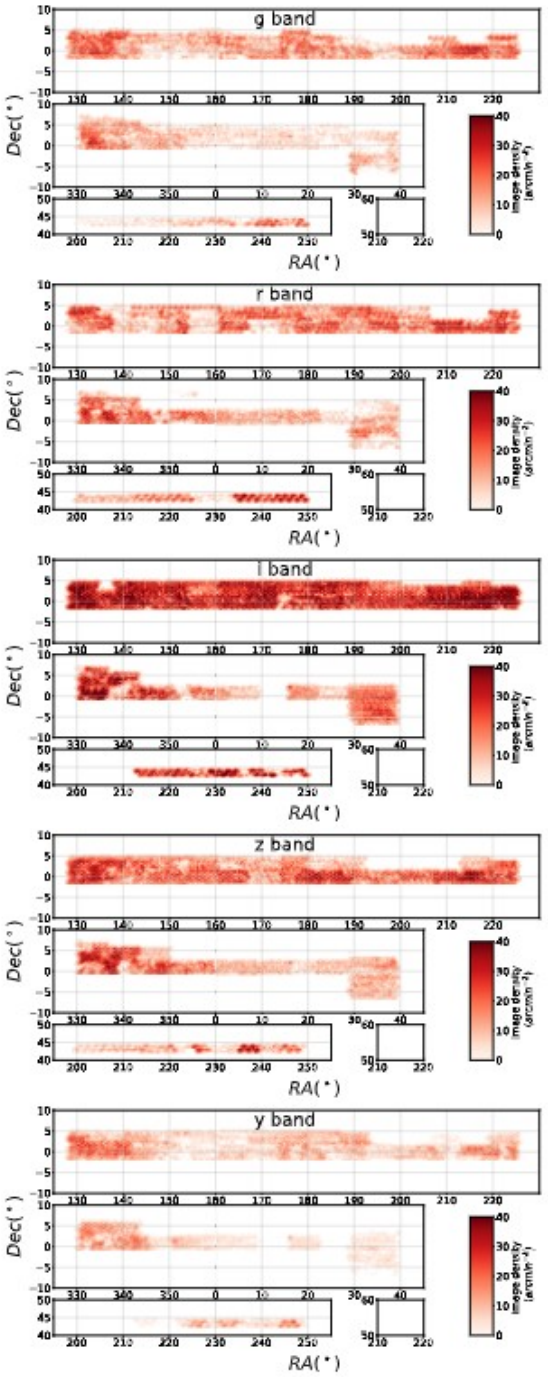


Liu et al., arXiv:2407.00370

HSC-DR3 Data Processing

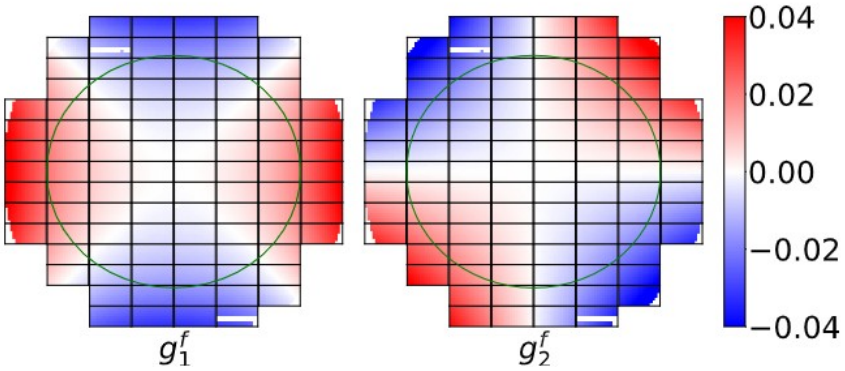
band	area	image density	galaxy density	shape noise
G	1343	8.33	7.68	0.421
R	1324	11.60	10.50	0.388
I	1314	22.28	19.33	0.361
Z	1350	13.84	11.93	0.376
Y	1220	6.40	5.66	0.428

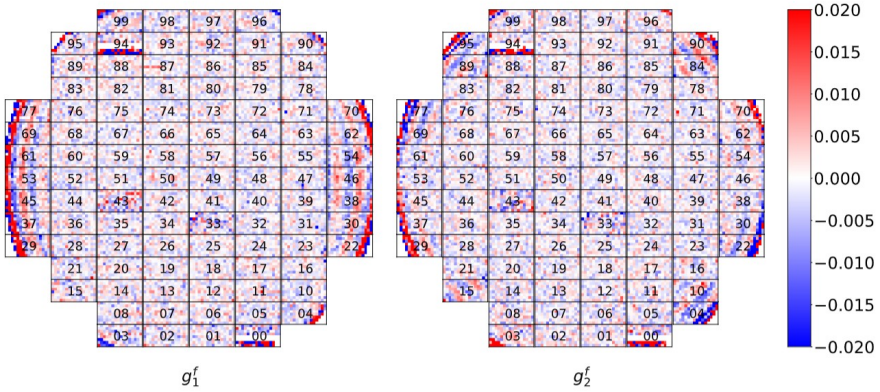


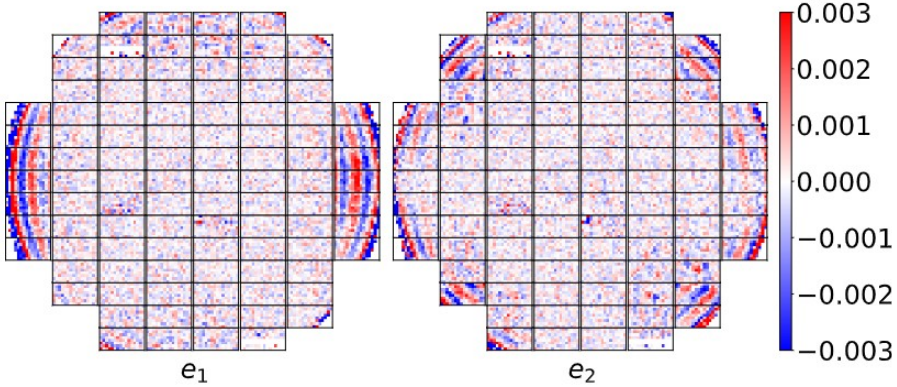


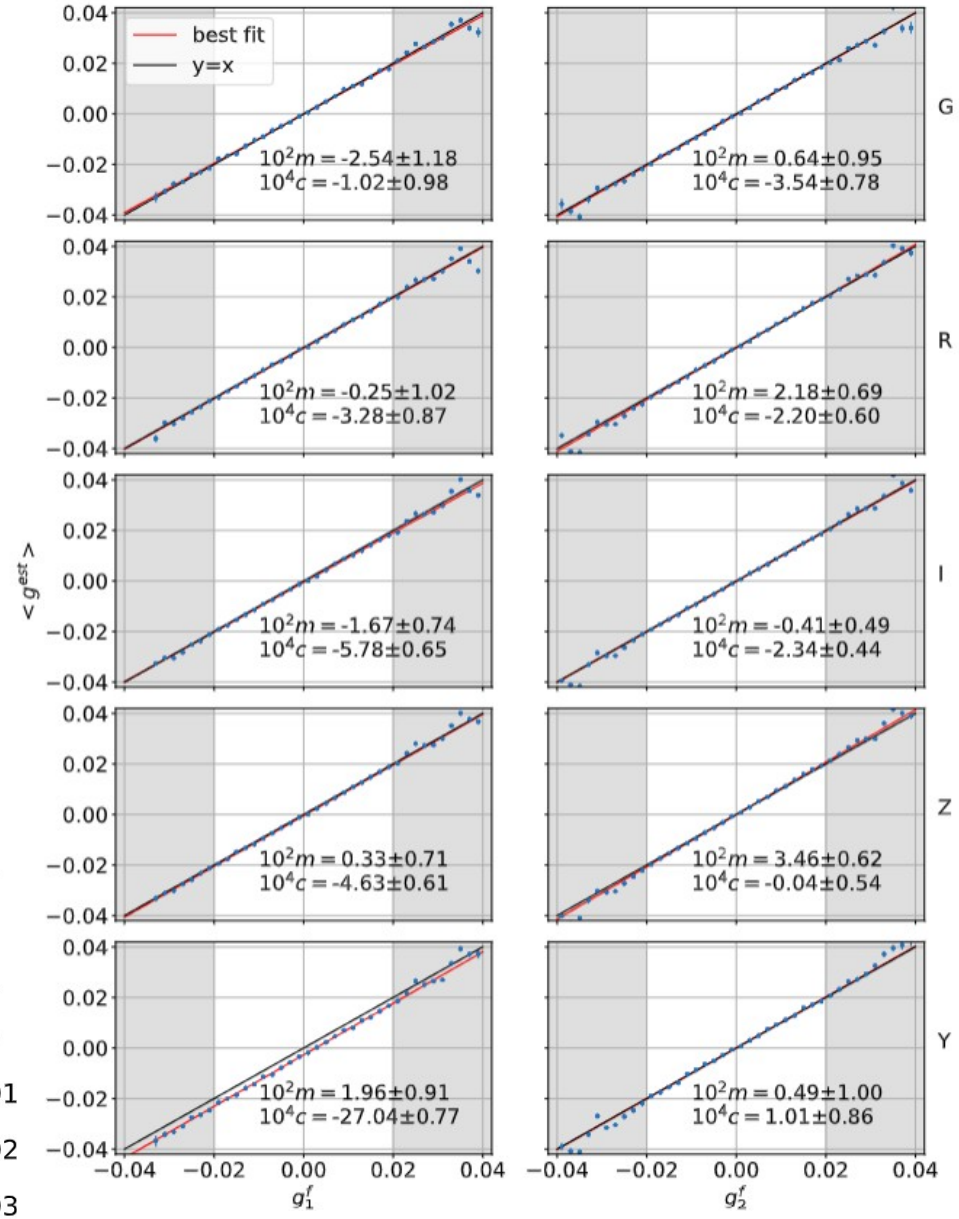
Field Distortion Test

$$g^{est} = (1+m)\,g^{f} + c$$



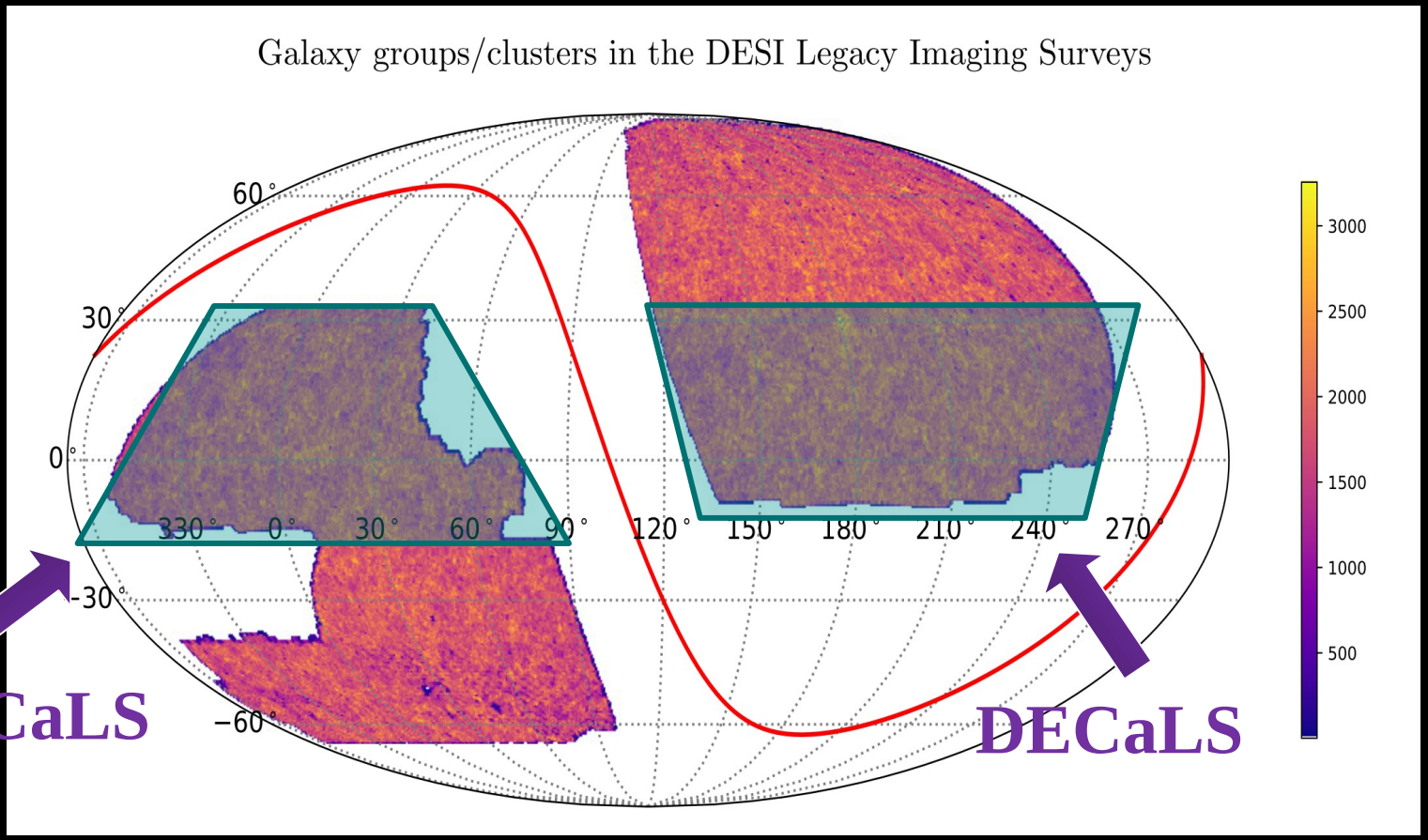






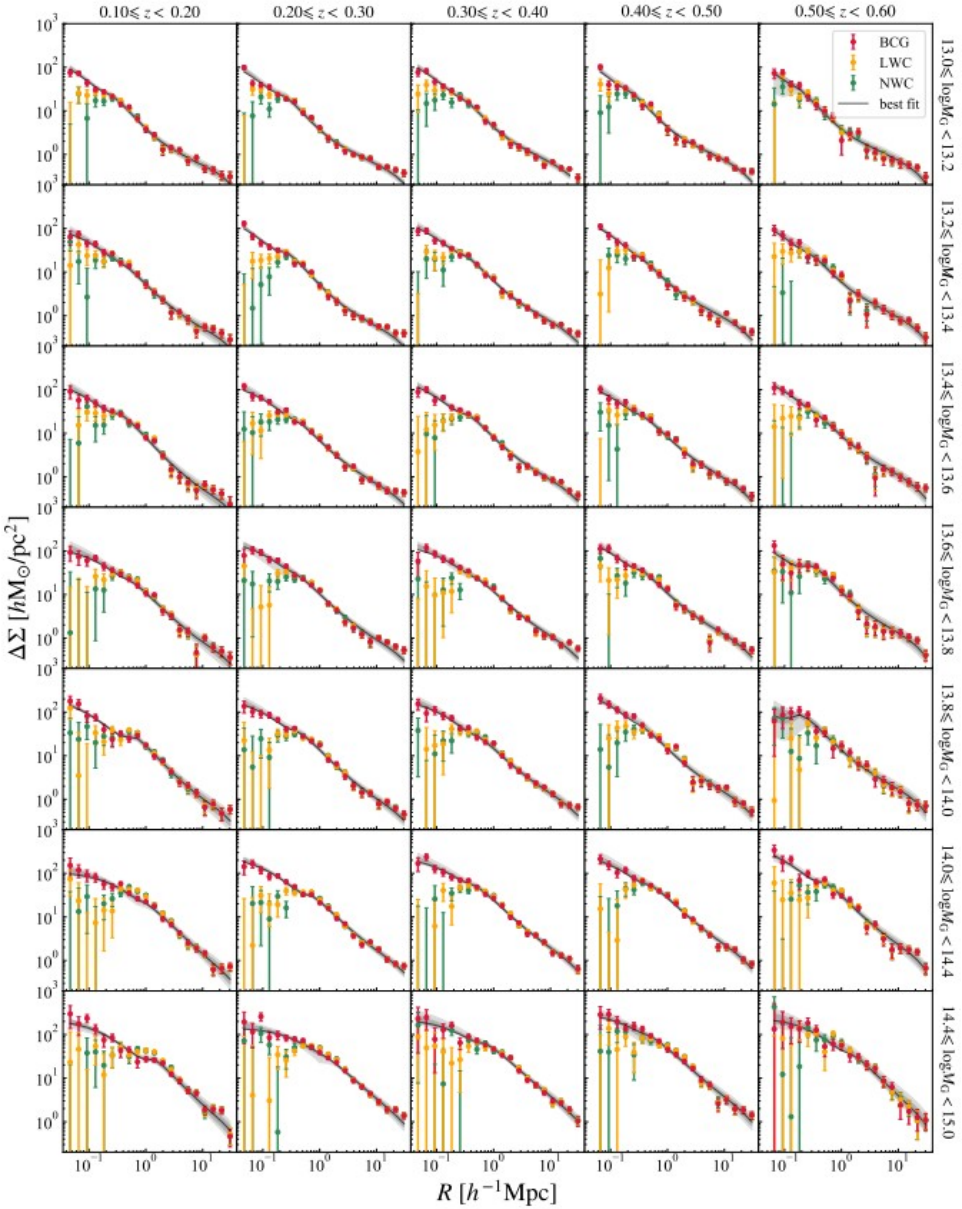
Halo Property & Cosmology with WL

https://gax.sjtu.edu.cn/data/DESI.html



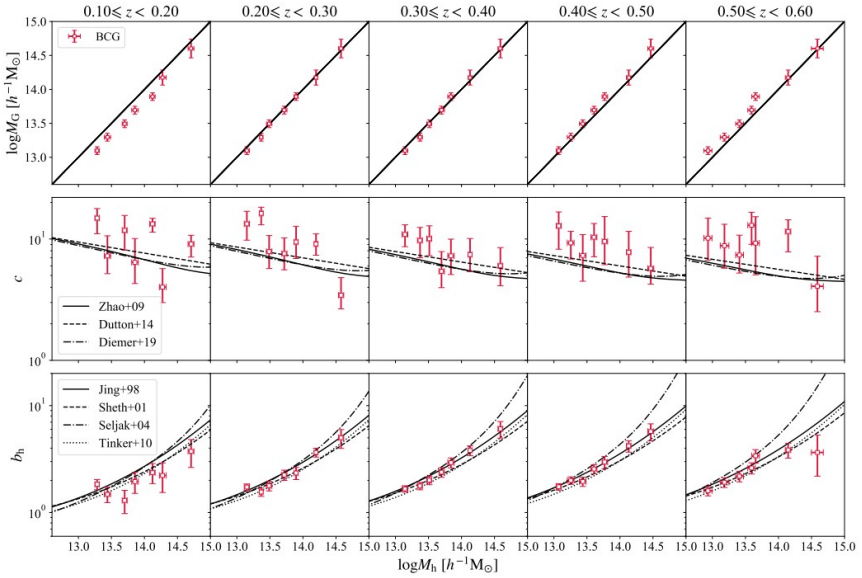
Region	Galaxies	Sky coverage	Groups Ng>=1	Ng>=3	Ng>=5	Ng>=10
NGC	69753872	9673	53335347	2750934	879844	200674
SGC	59598763	8580	45022007	2421063	795323	186841

Halo Property with WL





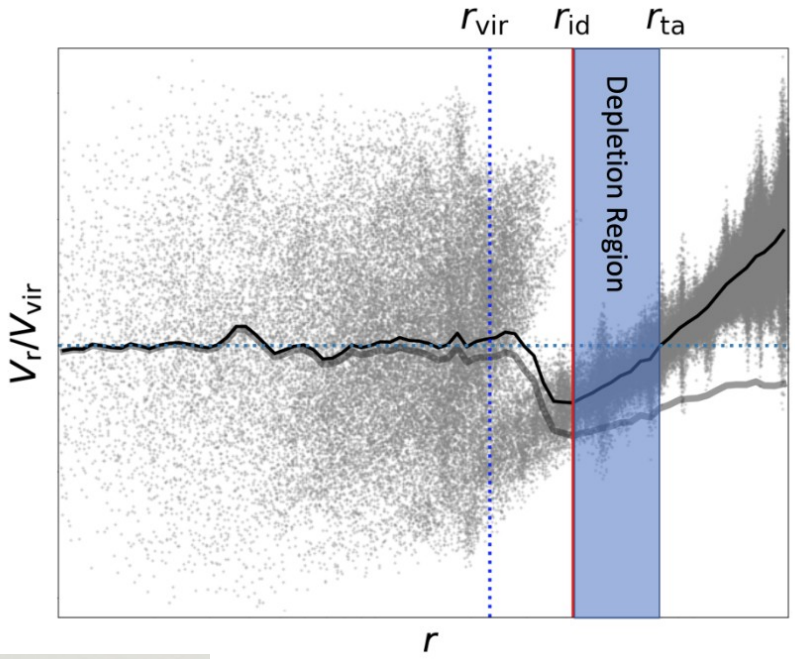
Jiaqi Wang

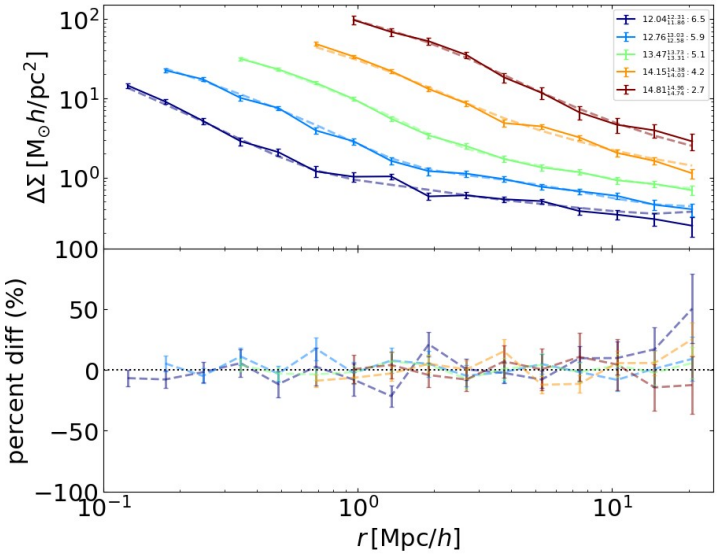


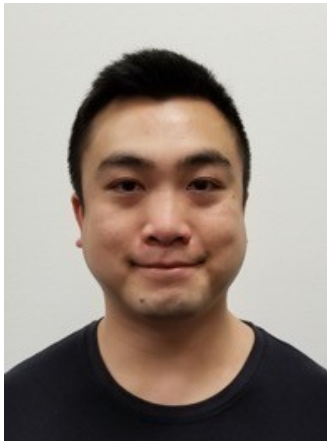
Wang et al. , 2022, ApJ, 936, 161

Probing the Halo Depletion Radius with WL

Agree with the Prediction from LCDM Simulation !



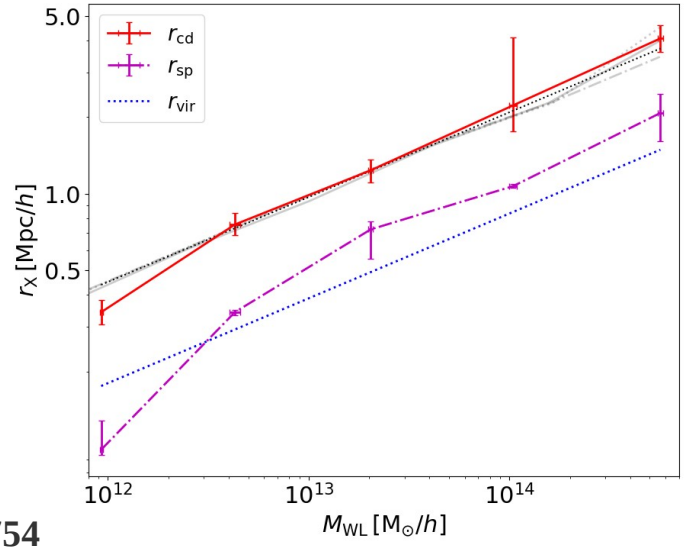




$$\rho(r) = \rho_m \times (b(r)\xi_{mm} + 1)$$

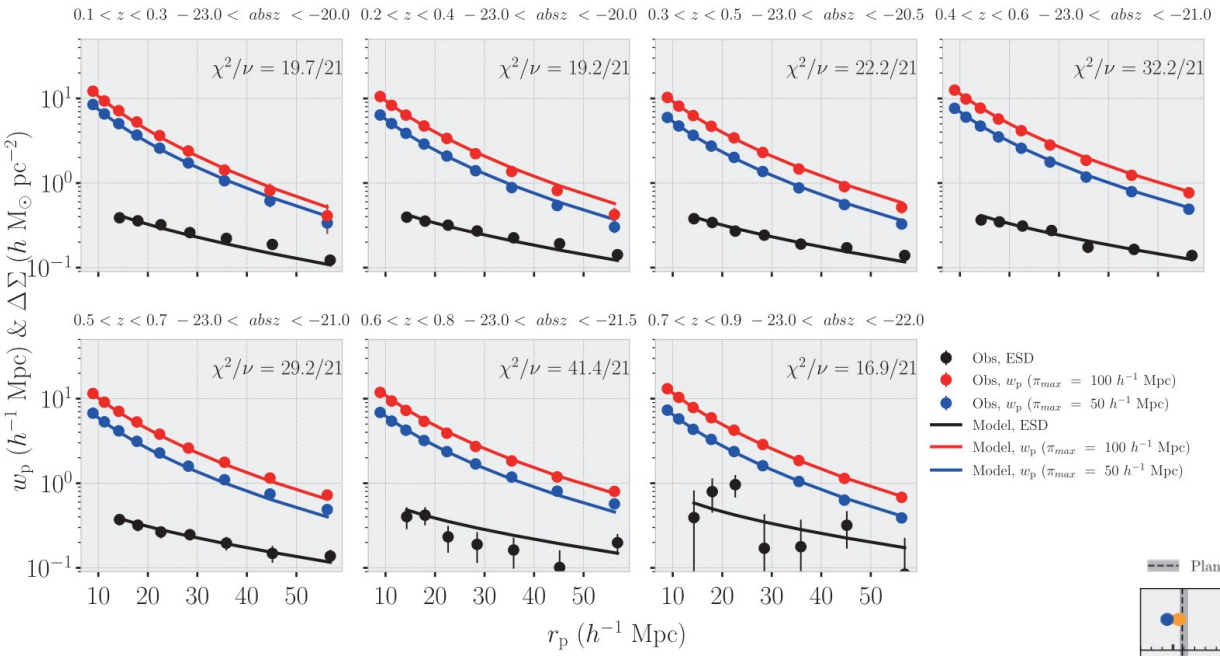
$$b^{Fit}(r) = \frac{1 + \left(\frac{r}{r_0}\right)^{-(\alpha+\beta)}}{1 + \left(\frac{r}{r_1}\right)^{-(\beta+\gamma)}} \times \left(b_0 + \left(\frac{r}{r_2}\right)^{-\gamma}\right)$$

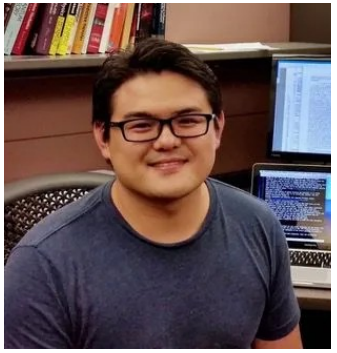
Matthew Fong



Fong, Han et al. , 2022, MNRAS, 513, 4754

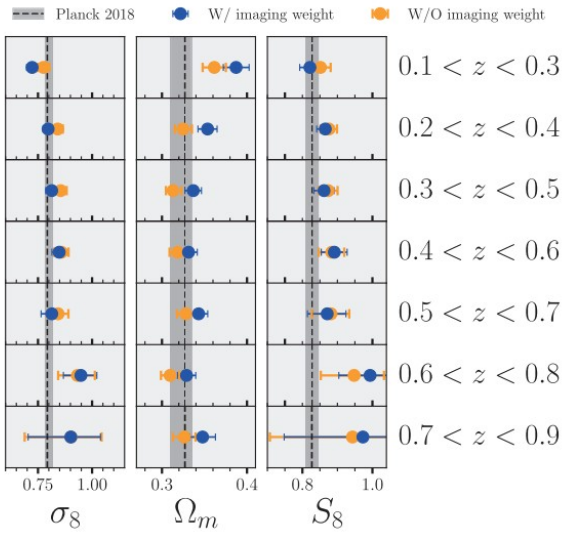
Cosmological Constraints from 2*2pt





Haojie Xu

By measuring the auto-correlation of the foreground LRG and their g-g lensing signals, we are able to place constraints on S_8.



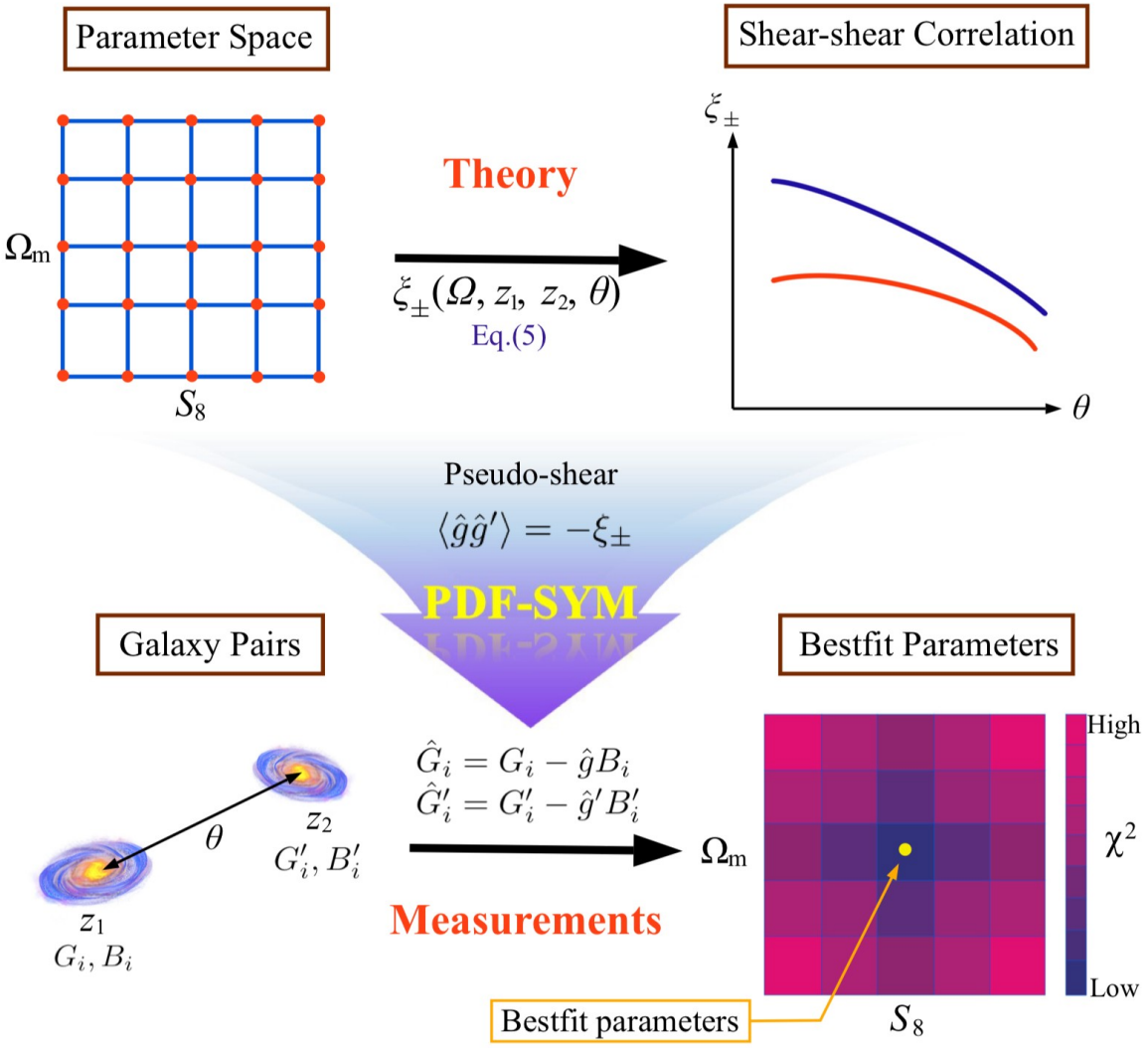
Xu et al. , 2023 , SCPMA , 66 , 12

Cosmological Constraints using Quasi-2D Shear-Shear Correlation

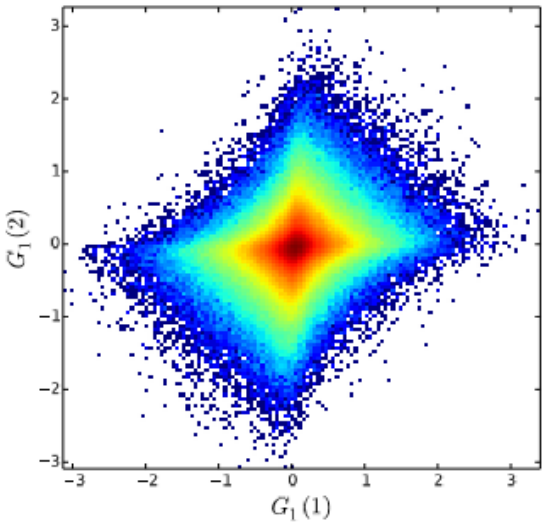


Zhenjie Liu

Quasi-2D:
1. using photo-z
2. no redshift binning



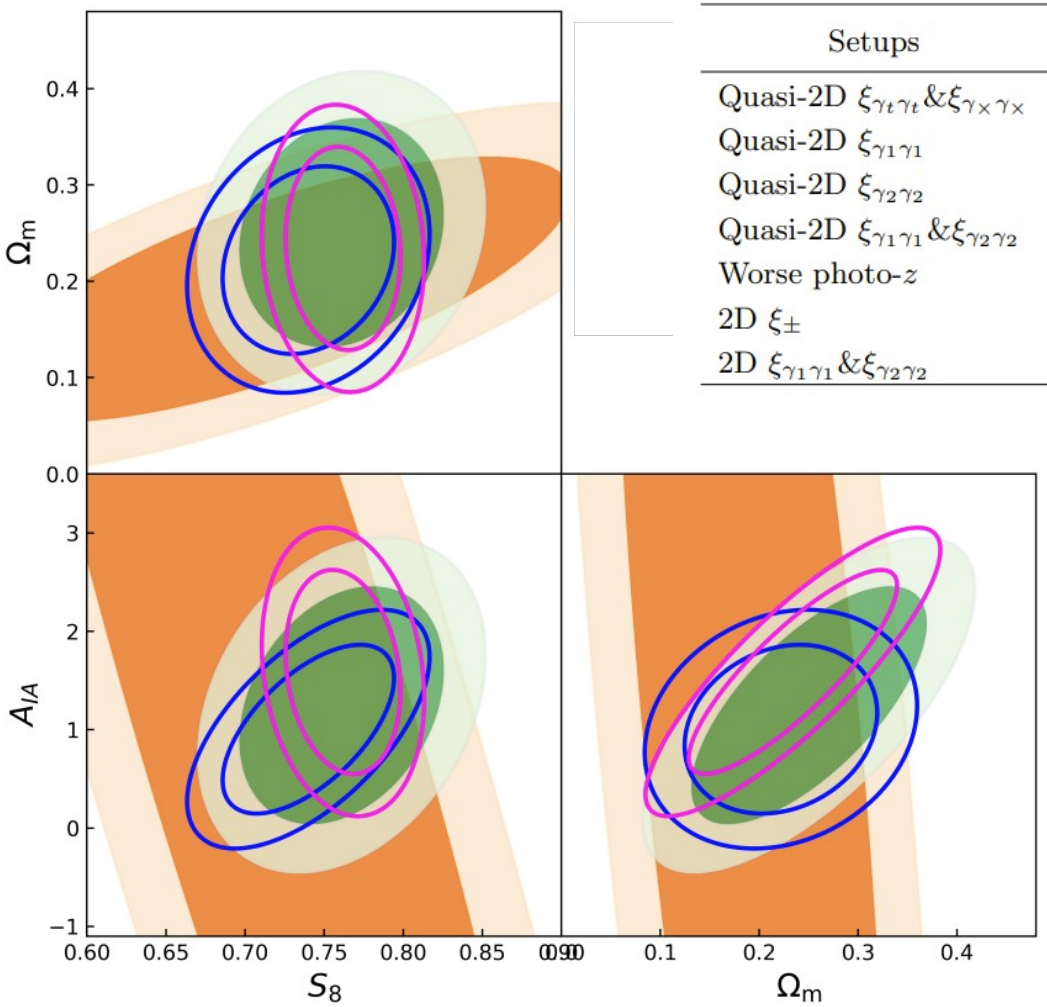
PDF-SYM method



Liu et al., arXiv:2310.11209

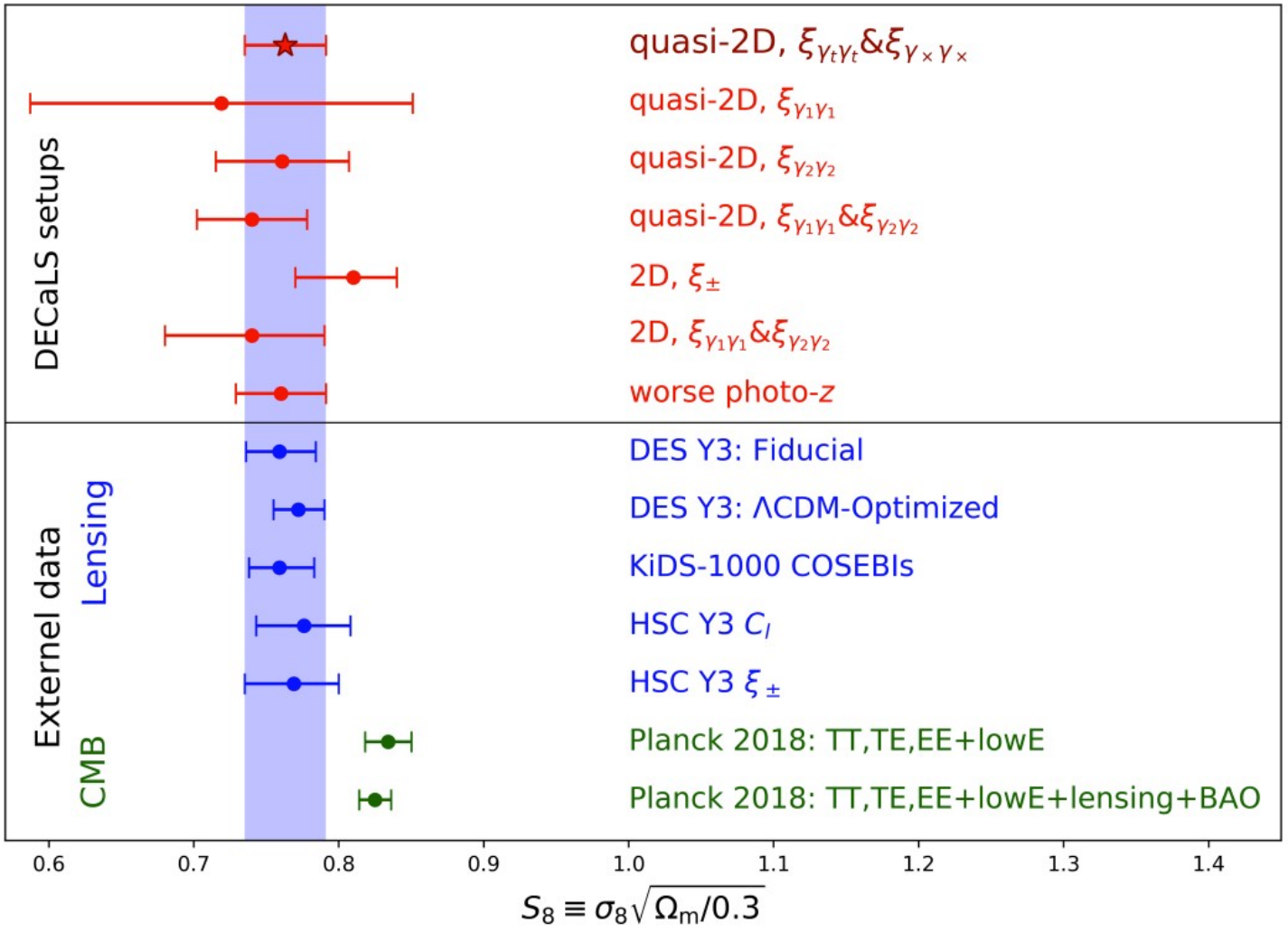
Cosmological Constraints from Different Types of Shear-Shear Correlations

Setups	S_8	$\Omega_{\rm m}$	$A_{\rm IA}$
Quasi-2D $\xi_{\gamma_t\gamma_t}\&\xi_{\gamma_\times\gamma_\times}$	$\mathbf{0.762 \pm 0.026}$	$\mathbf{0.23 \pm 0.07}$	$\mathbf{1.59 \pm 0.73}$
Quasi-2D $\xi_{\gamma_1\gamma_1}$	0.719 ± 0.132	0.19 ± 0.10	1.05 ± 6.43
Quasi-2D $\xi_{\gamma_2\gamma_2}$	0.761 ± 0.046	0.25 ± 0.08	1.25 ± 0.85
Quasi-2D $\xi_{\gamma_1\gamma_1}\&\xi_{\gamma_2\gamma_2}$	0.740 ± 0.038	0.22 ± 0.07	1.00 ± 0.60
Worse photo-z	0.761 ± 0.031	0.24 ± 0.06	2.37 ± 1.04
2D $\xi_\pm$	$0.81^{+0.03}_{-0.04}$	$0.25^{+0.06}_{-0.05}$	$2.47^{+1.35}_{-1.16}$
2D $\xi_{\gamma_1\gamma_1}\&\xi_{\gamma_2\gamma_2}$	$0.74^{+0.05}_{-0.06}$	$0.17^{+0.06}_{-0.05}$	$2.50^{+2.67}_{-2.01}$



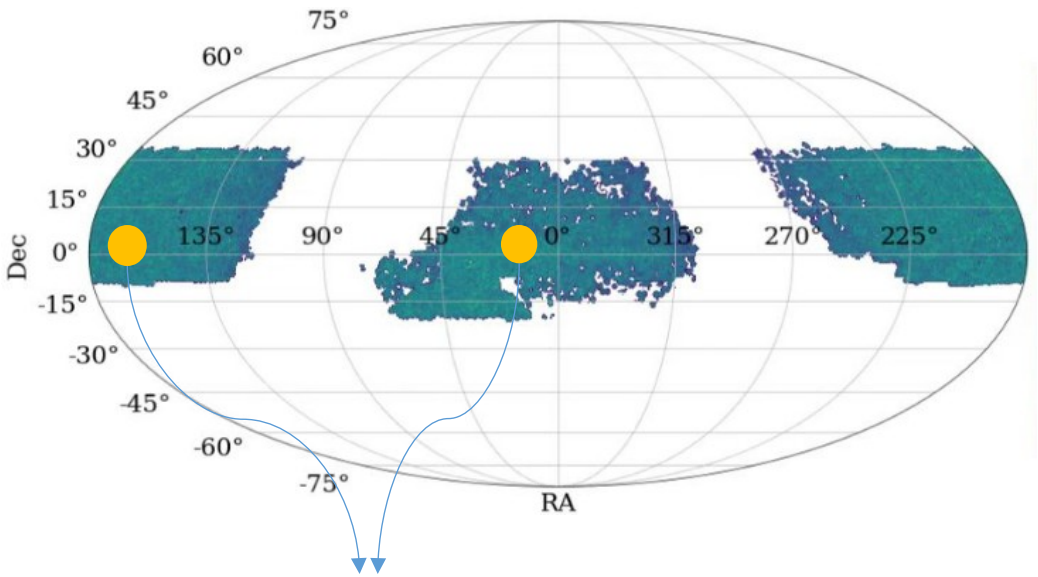
Liu et al., arXiv:2310.11209

Comparison with Other Results



Liu et al., arXiv:2310.11209

Tele-Correlation: a New Way to Calibrate Shear-Shear Correlation

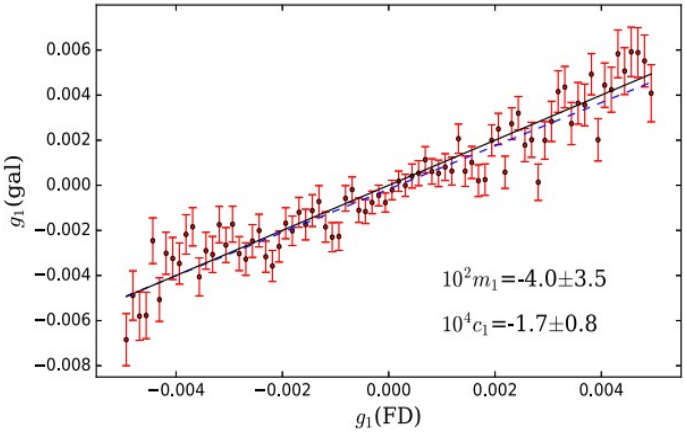




$$< g_1^A\, g_1^{A\prime} > = < (g_1^I + g_1 + g_1^f)(g_1^{I\prime} + g_1' + g_1^{f\prime}) >$$

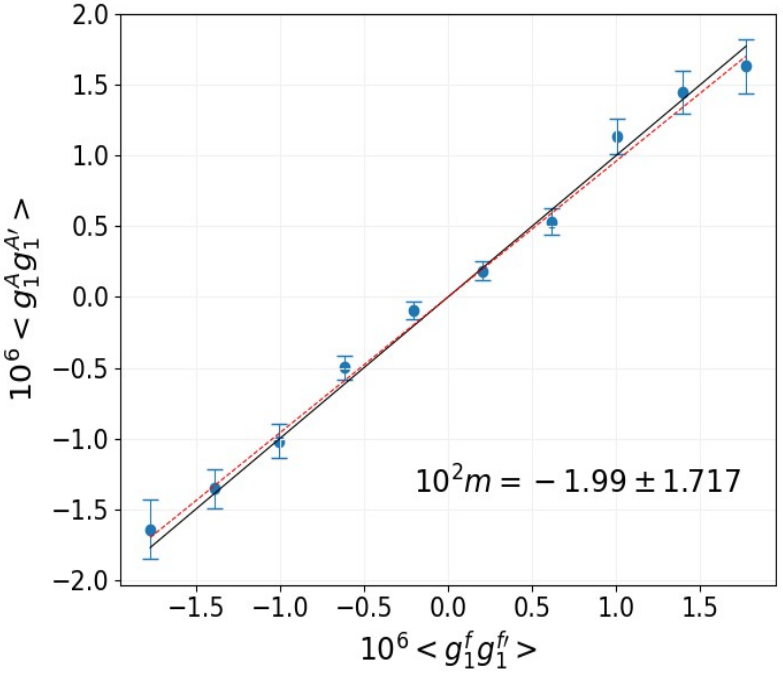
$$= < g_1^f g_1^{f\prime} > + < g_1^I g_1^{I\prime} > + < g_1 g_1' > + < g_1^I g_1' > + < g_1^{I\prime} g_1 >$$

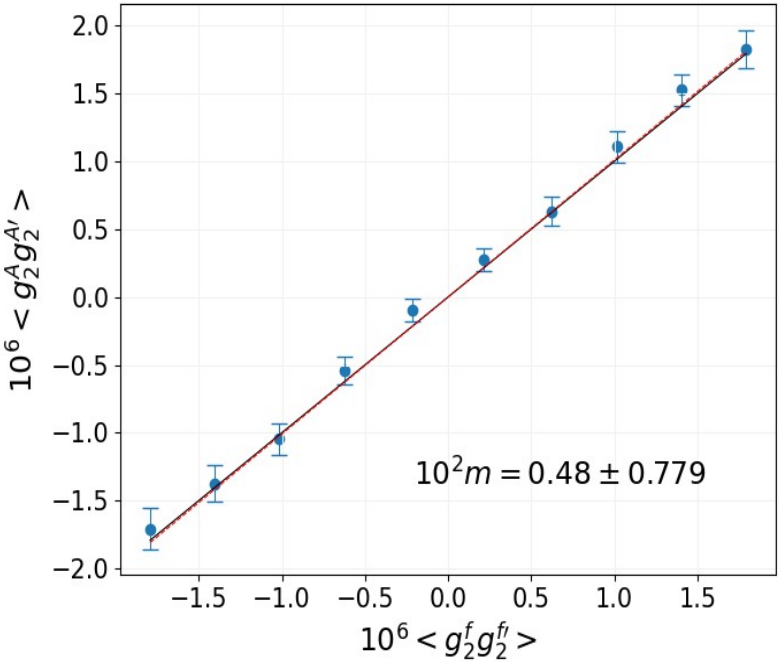
$$g_1^A\, g_1^{A\prime} = (1+m_1)^2 g_1^f\, g_1^{f\prime} + cc_1$$
$$g_2^A\, g_2^{A\prime} = (1+m_2)^2 g_2^f\, g_2^{f\prime} + cc_2$$



Shen et al., arXiv:2406.17991

Tele-Correlation Results for the Whole Sample

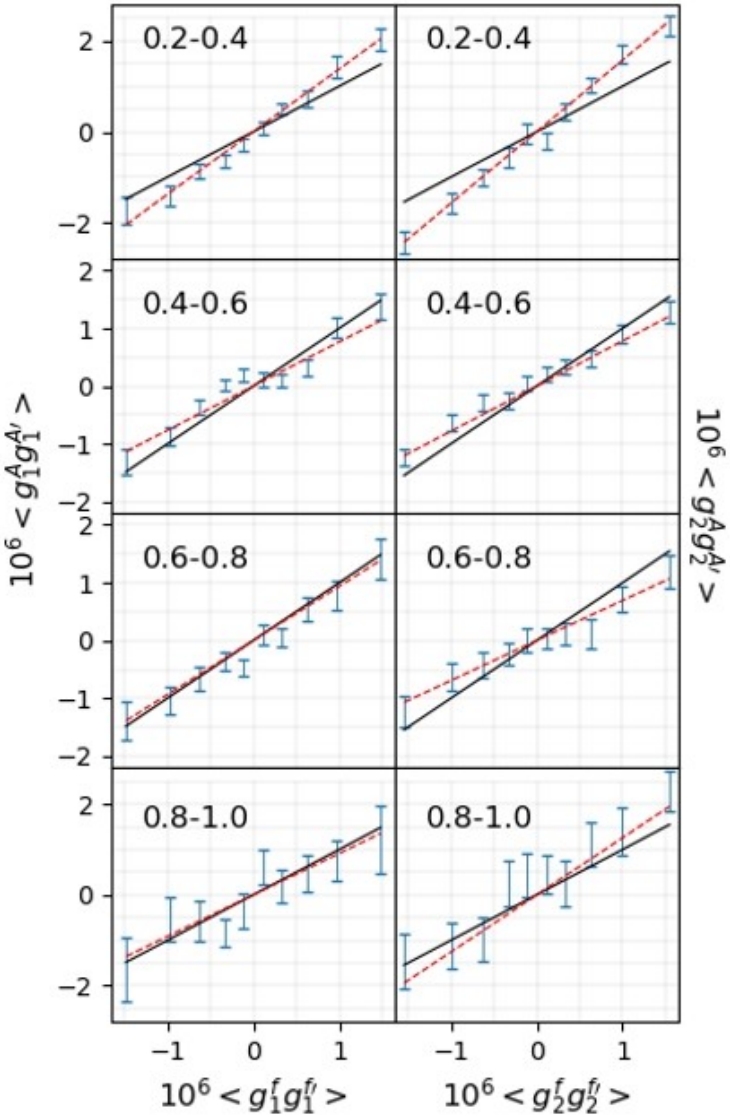




Tele-Correlation Results for Different Redshift Bins

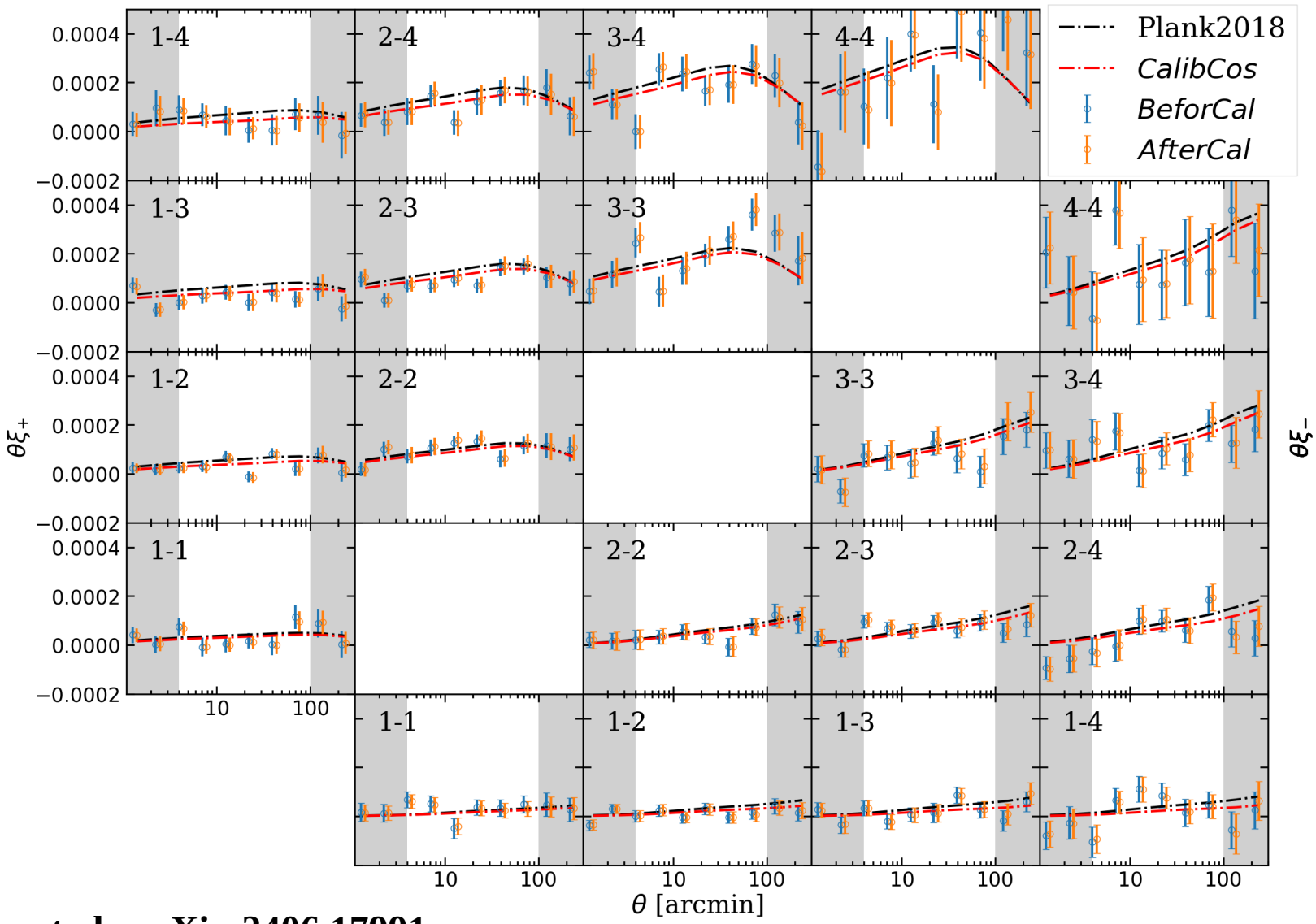
- **Including >130° galaxy pairs**

z	$10^2 \times m_1$	$10^8 \times cc_1$	$10^2 \times m_2$	$10^8 \times cc_2$
[0.1-∞]	**-2.0±1.72**	4.1±2.6	**0.5±0.78**	6.4±1.53
[0.2-0.4]	**17.5 ± 3.02**	-5.2±3.71	**25.6 ± 3.26**	-3.6±5.26
[0.4-0.6]	**-11.8 ± 5.34**	7.0±6.69	**-10.9 ± 1.61**	2.1±2.54
[0.6-0.8]	**-3.2 ± 3.84**	-14.4±4.70	**-15.4 ± 2.70**	-3.3±4.04
[0.8-1.0]	**-4.3 ± 8.72**	-8.5±11.30	**12.9 ± 5.51**	25.6±9.45



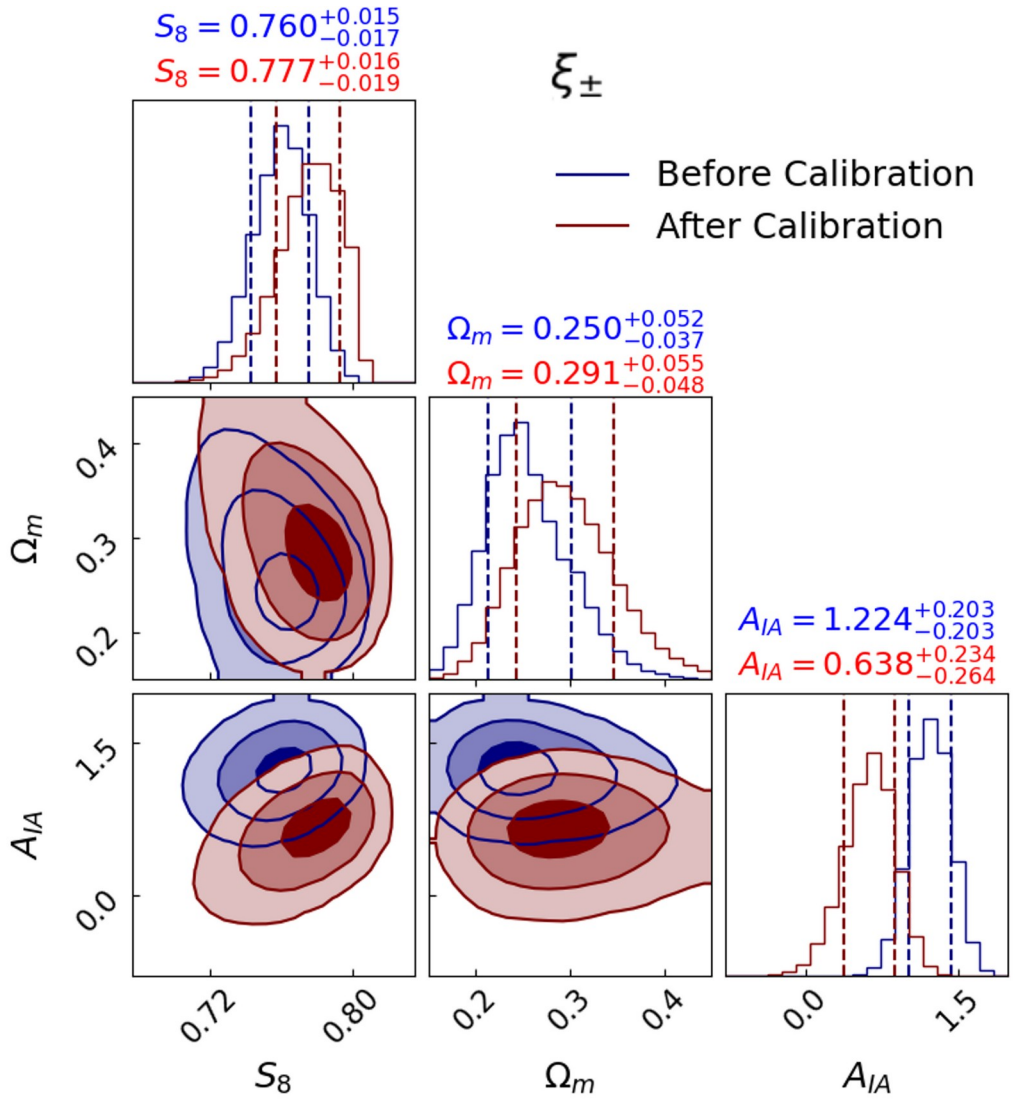
Quite Obvious Multiplicative Biases！

3D Shear Tomography Results



Shen et al., arXiv:2406.17991

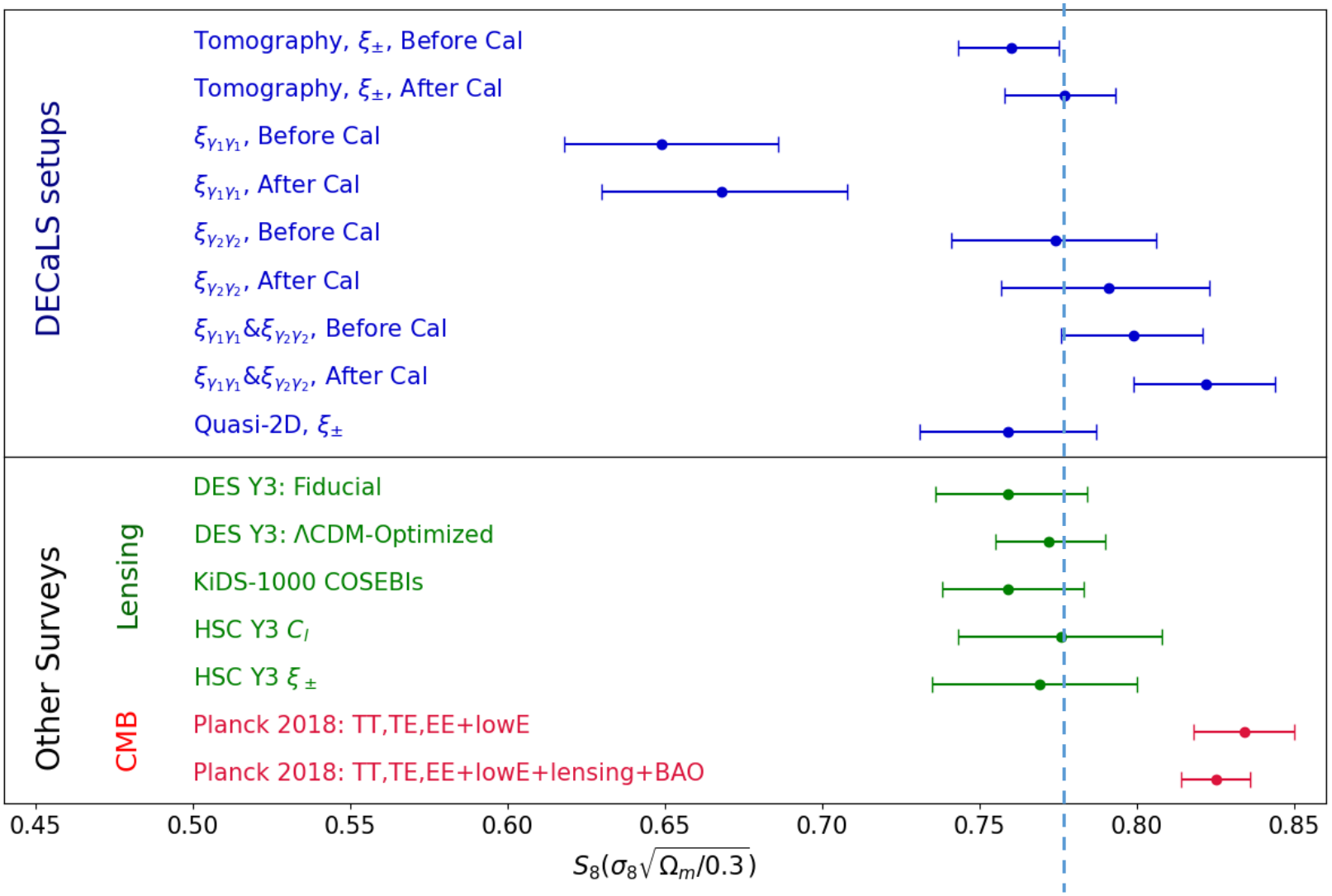
3D Shear Tomography Results





Zhi Shen

3D Shear Tomography Results



Outline:

- Motivation & Thoughts
- Recent Progress
- Conclusions

Conclusions

- **Based on the Fourier_Quad shear measurement method, we have developed a fast and accurate data processing pipeline, taking care of all major steps in shear measurement;**
- **We have applied the pipeline to the CFHTLenS, DECaLS, HSC imaging data. The resulting shear catalogs show very high accuracy verified by the field-distortion test. The shear catalogs cover more than 10000 square degrees;**
- **We have used our shear catalog to measure the dark matter halo properties (mass function, bias, c-M relation, depletion radius), and the results are in very good agreement with simulation results;**
- **For 2*2pt (g-g lensing + g-g corr), our constraints on S_8 is similar to the CMB result. For the shear-shear correlation, our constraint on S_8 has about 2σ tension with the CMB value;**
- **Although weak lensing measurement is difficult in general, some key problems are tractable, deserving model-independent treatment;**
- **Our shear catalog is accessable via** https://gax.sjtu.edu.cn/data/DESI.html.

Collaborations are very welcome!